UNIVERSITÀ DEGLI STUDI DI TRIESTE

XXIX CICLO DEL DOTTORATO DI RICERCA IN

BIOMEDICINA MOLECOLARE

SIGNIFICANCE OF $p27^{kip1}$ IN GROWTH AND RESPONSE TO THERAPY OF LUMINAL BREAST CANCER

Settore scientifico-disciplinare: BIO/11 BIOLOGIA MOLECOLARE

DOTTORANDA
MARTINA CUSAN

COORDINATORE
PROF.SSA GERMANA MERONI

SUPERVISORE DI TESI
PROF. GUSTAVO BALDASSARRE

CO-SUPERVISORE DI TESI
DOTT.SSA BARBARA BELLETTI

ANNO ACCADEMICO 2015/2016

Università degli Studi di Trieste

School in MOLECULAR BIOMEDICINE

PhD Thesis

SIGNIFICANCE OF $p27^{kip1}$ IN GROWTH AND RESPONSE TO THERAPY OF LUMINAL BREAST CANCER

PhD student
Martina Cusan

Supervisor
Gustavo Baldassarre

Co-supervisor
Barbara Belletti

PhD coordinator
Germana Meroni

XXIX cycle – Academic Year 2015-2016

Abstract

The CDK inhibitor $p27^{kip1}$ is frequently down modulated in breast cancer (BC) and mutations in its gene, CDKN1B, have been recently identified as driver genetic lesions, almost exclusively in luminal BC (LBC). Clinical studies have recognized $p27^{kip1}$ expression as predictive of outcome for LBC patients. Resistance to therapy and disease relapse are unfortunate events that occurs frequently, especially in patients carrying the luminal B subtype of BC.

We thus hypothesized that elucidating the role of $p27^{kip1}$ and its mutations in LBC progression and response to treatments could contribute to ameliorate the clinical management of this disease.

To this aim, we genetically manipulated the MCF-7 luminal B BC cell line to Knock-Out $p27^{Kip1}$ gene and Knock-In $p27^{Kip1}$ mutants, exploiting the Zinc Finger Nucleases technology. We explored the impact of modified expression $p27^{Kip1}$ on MCF-7 cell behavior in different experimental settings. Tumorigenic and stem-like features were increased by loss of $p27^{Kip1}$ and by expression of the mutants. Next, we tested the response of these clones to radiotherapy, which represents an integral part of the gold standard treatment for LBC patients. We irradiated MCF-7 clones and evaluated their survival rates by clonogenic assay. Our data clearly demonstrate that loss of $p27^{Kip1}$ conferred radioresistance to MCF-7 cells. In particular, analyses of H2AX foci and aberrant mitoses highlighted that loss of $p27^{Kip1}$ affected DNA damage repairing ability and significantly increase the presence of mitotic defects in surviving cells.

In conclusion, during my PhD thesis we have generated tools for studying the role of $p27^{Kip1}$ in LBC, *i.e.* MCF-7 luminal B BC cells Knock-Out for $p27^{Kip1}$ and Knock-In for mutants that have been described in human LBC patients. Moreover, we have observed that loss $p27^{Kip1}$ conferred augmented tumorigenicity, self-renewal potential and radioresistance to luminal B BC cells, suggesting a critical role for $p27^{Kip1}$ in the maintenance of genomic stability.

Table of contents

List of abbreviations

BC	Breast cancer
LBC	Luminal breast cancer
DCIS	Ductal carcinoma in situ
KO	Knock-Out
KI	Knock-In
WT	Wild-type
ER	Estrogen receptor
PR	Progesteron receptor
HER2	Human epidermal growth factor receptor 2
DSB	DNA double-strand break
DDR	DNA damage response
ATM	Ataxia telangiectasia mutated kinase
AIs	Aromatase inhibitors
G1	Gap phase 1
G2	Gap phase 2
53BP1	p53-binding protein 1
BRCA1	breast cancer 1
FGFR1	Fibroblast growth factor 1 receptor
IGFR1	Insulin-like growth factor 1 receptor
CHK2	Checkpoint effector kinase 2
CDK	Cyclin dependent kinase
CKI	CDK inhibitor
ZFN	Zinc Finger Nucleases
OS	Overall survival
DFS	Disease-free survival
RFS	Relapse-free survival
NHEJ	Non homologous end-joining
HDR	Homology directed repair

1 Introduction

1.1 Breast cancer

Breast cancer (BC) is the most common malignancy in women. BC is the second cause of cancer death among women in more developed regions and ranks as the most frequent in women in less developed regions (Ferlay et al., 2015).

In the last two decades, mortality rates have generally remained stable or decreased in North America and the European Union (EU). It is estimated that one in eight to ten women will get BC during their lifetime and in 2016 mortality from BC in the EU is expected to drop by 8%. This decrease is mostly attributable to early detection due to the implementation of screening/prevention programs and efficient systemic therapies (Harbeck and Gnant, 2016).

BC is a highly heterogeneous disease under several viewpoints: histological features, genomic pattern, response to different therapeutic options and clinical outcome.

Histologically, the most common BC types are the ductal and lobular carcinomas, which account for more than 80% of all BC in the western world. Among these types, the *in situ* and the invasive ductal carcinoma represent the most common subtypes. Ductal carcinoma in situ (DCIS) refers to a condition where abnormal cells replace the normal mammary epithelial cells of the ducts and may greatly expand into the ducts and lobules. DCIS is considered a noninvasive form of BC because the abnormal cells have not grown beyond the layer of cells where they originated. Since there is no certain way to determine the progressive potential of a DCIS lesion, surgery and sometimes γ-radiation and/or hormonal therapy is the usual course of action following a diagnosis of DCIS. Most BCs are invasive, or infiltrating. These cancers have broken through the walls of the glands or ducts where they originated and have grown into the surrounding tissue. The prognosis of invasive BC is strongly influenced by the stage of the disease (American Cancer Society, 2015).

BC is also divided in subtypes defined by genetic profiles. These subtypes have different epidemiological risk factors, different natural histories and different responses to systemic and local therapies (Goldhirsch et al., 2011). By using a hierarchical clustering analysis of gene expression profiling, Perou et al. have established five BC intrinsic subtypes with distinctive biological and clinical features: Luminal A, Luminal B, HER2-enriched, Claudin-low, Basal-like (Perou et al., 2000; Sorlie et al., 2001, 2003). However, gene expression profiling technique is a costly and complicated process that still does not represent a standard practice.

Pathologists and clinicians stratify BC in three major tumor subclasses with major therapeutic implications, according to their receptors expression status: Estrogen (ER) and Progesterone (PR) receptors expressing tumors, Human Epidermal growth factor Receptor 2 (HER2) overexpressing tumors, triple-negative tumors, due to lack of or low positivity for ER, PR and HER2 (Goldhirsch et al., 2011; Higgins and Baselga, 2011; Viale, 2012). It's important to underline that the molecular subtypes are divided following hormone receptors expression, validating the more convenient approximation using the routinely evaluated biological markers ER, PR, and HER2 (Brenton, 2005; Goldhirsch et al., 2011).

Among the ER-positive tumors, two major subtypes, luminal A and luminal B, have been identified. Although both are hormone receptor expressing, these two subclasses have distinguishing characteristics that will be discussed in a section below. In general, the luminal subtypes carry a good prognosis and BC patients with positive ER, PR and HER2 status are responsive to targeted therapeutics given as monotherapy, or in combination with chemotherapy (Goldhirsch et al., 2011; Higgins and Baselga, 2011).

Among the ER-negative tumors, the major subtypes are the HER2-enriched subtype and the triple-negative subtype. Both subclasses have a poorer prognosis. HER2-enriched subgroup shows elevated expression not only of HER2 but also of many other genes residing near HER2 in the genome. For HER2 positive BC, a growing number of HER2-targeted agents have become available, including Trastuzumab, Lapatinib and Pertuzumab (Mohamed et al., 2013). The triple-negative BC class includes Claudin-low and Basal-like molecular subtypes and display high proliferative rate compared with other subtypes. They are characterized by lack of ER and related genes expression, low expression of HER2 and strong expression of basal cytokeratins 5, 6, and 17 and proliferation-related genes. Given its triple-negative receptor status (ER, PR, and HER2), Basal-like BC is not amenable to conventional targeted therapies for BC such as endocrine therapy or Trastuzumab, leaving only chemotherapy in the therapeutic armamentarium (Brenton, 2005; Goldhirsch et al., 2011; Higgins and Baselga, 2011).

1.2 Luminal Breast Cancer

Luminal BC (LBC) are the most common subtype of BC, accounting more than 60% of all diagnosed BC worldwide (Ades et al., 2014). Among the BC, they are the most heterogeneous in terms of gene expression, mutation spectrum, copy number changes and patient outcomes (Koboldt et al., 2012).

Molecular profiling studies have found that this ER-positive breast tumor type comprised at least two distinct diseases with differing biology, defined as luminal A and luminal B BC subtypes (Creighton, 2012). Both subclasses have expression patterns reminiscent of the luminal epithelial component of the breast, including expression of cytokeratins 8/18, GATA3, FOXA1, MYB, ER and genes associated with ER activation such as CCND1 (Koboldt et al., 2012; Tran and Bedard, 2011). Luminal A tumors are characterized by the high expression of ER-related- and low expression of proliferation-related-genes. Patients with luminal A BC have a good prognosis, the relapse rate is significantly lower than the other subtypes and treatment is mainly based on hormonal therapy, such as Tamoxifen and Aromatase Inhibitors (Goldhirsch et al., 2011; Higgins and Baselga, 2011).

Luminal B cancers showed lower expression of ER as well as low expression of PR genes and higher expression of proliferation genes, like MKI67, and cell cycle–associated genes, like CCND1, CCNB1 and MYB (Ades et al., 2014; Creighton, 2012; Koboldt et al., 2012).

The Cancer Genome Atlas (TCGA) Network initiative characterized a high number of primary BC using a wide variety of platforms. They showed that in luminal B BC loss of ATM and MDM2 amplification are events occurring frequently. Moreover, respect luminal A, luminal B BC have lower frequency of PIK3CA mutations (29% vs. 45%) and higher frequency of TP53 mutations (29% vs. 12%) (Ades et al., 2014; Koboldt et al., 2012). In LBC, phosphatidylinositol-3-kinase (PI3K) activation is implicated in *de novo* and acquired endocrine resistance (Miller et al., 2011). Despite lower frequency of PIK3CA mutations (Chang et al., 2013), luminal B cancers have higher PIK3 activation than luminal A (Loi et al., 2010). Through whole genome analysis, Ellis and colleagues found other significantly mutated genes considered to be related with endocrine therapy sensitivity, such as GATA3, RUNX1, CBFB and CDKN1B. GATA3 was found to be mutated with significant degree in both luminal A and B subtype with a similar frequency (~15%) but in different ways: luminal A displayed hotspot CA intron 4 deletions associated, while exon 5 frame shifts were ascribed in luminal B cancer (Ades et al., 2014; Ellis et al., 2012). Of note, mutations in GATA3 has been proved to be a positive predictive marker for endocrine treatment response (Jiang et al., 2014; Yoon et al., 2010). RUNX1 loss-of-function

mutations affecting its expression, and its dimerization with its partner CBFB, has been associated with the luminal B subtype and endocrine resistance (Ellis et al., 2012). With regard to the tumor suppressor gene CDKN1B, two different truncating mutations were identified and only in luminal subtypes (Ellis et al., 2012; Spirin et al., 1996). CDKN1B encodes for the cell cycle inhibitor $p27^{kip1}$ and functional studies demonstrated that high $p27^{kip1}$ expression predicts sensitivity to endocrine- and chemo-therapy in LBC patients (Pohl, 2003; Porter et al., 2006), while $p27^{kip1}$ downregulation has been associated with resistance to radiotherapy (Payne et al., 2008) and anti-HER2 therapies (Lee-Hoeflich et al., 2011; Nahta, 2004; Zhao et al., 2015). The implications of $p27^{kip1}$ in LBC will be discussed in sections below.

Luminal B BC has in general a poorer outcome compared with the counterpart luminal A subtype. Overall survival in untreated luminal B BC is similar to the Basal-like and HER2-positive subgroups, which are widely recognized as high-risk subtypes. The increased relapse risk associated with the luminal B phenotype appears to be limited to the early period after surgery. Given that increased proliferation is characteristic of luminal B cancer, it is not surprising that increased relapse rates observed in this luminal subtype are confined to the first 5 years after diagnosis, with no difference in distant relapse beyond 5 years (Tran and Bedard, 2011). There are differences in the anatomic sites of relapse according to molecular subtypes, with LBC appear to have a predilection for bone and pleura metastasis. However, in a small study of 81 patients with metastatic BC, no differences in metastasis sites were observed between luminal A and B BC (Smid et al., 2008).

1.3 Therapeutic treatments for Luminal Breast Cancer patients

Multiple therapies are available for the treatment of LBC. The choice of the type of surgery, drug treatment and/or γ-radiation, depends on the state of tumor progression and its histological and molecular characteristics.

1.3.1 Surgery

Local surgery is in general the first treatment that BC patients receive. Surgical treatment could consist in breast-conserving surgery or mastectomy. When possible, it is preferred a conservative surgery, that is partial mastectomy or lumpectomy, where is excised only the nodule with a small area of the surrounding tissue (tumor margin). In case that the disease is too much extended is practiced a radical mastectomy, which consist in the removal of the entire breast. Both breast conserving surgery and mastectomy are usually accompanied by removal of one or more regional lymph nodes from the axilla to determine if the disease has spread beyond the breast. This helps stage the cancer and determine the subsequent therapies (American Cancer Society, 2015; Linee Guida AIOM 2015).

1.3.2 Γ-radiation therapy

Surgery aims to remove any disease that has been detected in the breast and regional lymph nodes. Surgery does not, however, remove undetected occult cancer cells that may remain within the breast, scar, chest wall or remaining lymph nodes. These microscopical tumor residues may lead to local recurrence and also to distant metastases. Administration of radiotherapy has been shown to minimize these events after BC surgery and it is thus used as standard adjuvant treatment of early BC (Budach et al., 2015; Langlands et al., 2013).

1.3.2.1.1 The DNA damage response after γ-radiation

Γ-γ-radiation damages cells by many mechanisms, the most important in tumor cell killing is DNA damage. This damage can occur due to direct effect of γ-radiation on DNA molecules (30-40% of lesions) or by generation of free radicals that in turn damage DNA (60-70% of lesions). The most lethal lesion is the DNA double-strand breakage. The generation of double-strand breaks (DSBs) triggers sophisticated and highly regulated DNA damage response and repair (DDR) pathways. Because high-fidelity replication of the genome is critical to appropriate cellular division, successful repair of DNA lesions will allow the cell to continue in the cell cycle. Unsuccessful repair can trigger the death of the

damaged cells, and uncorrected repair will generate mutations that can lead to cell resistance to radiotherapy (Santivasi and Xia, 2014). Cancer cells DDR is different from that of normal cells, primarily because most (if not all) cancers will have lost one or more DDR pathway or capability during their generation, leading to a greater dependency on the remaining pathways. So, DDR processes may hold the key to determining tumor responses to radiotherapy (O'Connor, 2015).

Following DSBs formation, the histone H2AX is rapidly phosphorylated on its serine residue 139 (γH2AX) by ataxia telangiectasia mutated (ATM) kinase, a member of the phosphatidylinositol-3-OH kinase family. γH2AX formation occurs within minutes after damage, and extends for up to 1-2 megabases from the site of the break in the DNA. The biological function of γH2AX foci is to shelter the broken DNA ends from decay and prevent illegitimate repair processes, to amplify the DNA damage signal and to provide a platform for subsequent DNA repair protein recruitment (Kinner et al., 2008). MDC1 (DNA damage checkpoint 1), the major protein to localize to the sites of DNA breaks, orchestrates the recruitment of the MRN complex (formed by the protein MRE11, RAD51, NBS1) and many DNA damage repair proteins, including 53BP1 (p53-binding protein 1) and BRCA1 (breast cancer 1). These complex of proteins that "sense" the DNA damage activate an intricate signal transduction cascade that induce cell cycle arrest, creating an extended time window to allow completion of lesion removal prior to replication or cell division. ATM phosphorylates the cell cycle inhibitor $p27^{Kip1}$ (Cassimere et al., 2016) and the checkpoint effector kinase CHK2, which can prevent replication of damaged DNA by activating p53 and p21, which results in G1/S cell cycle checkpoint arrest. Alternatively, CHK2 can arrest the cell cycle at the intra S phase delaying replication origin firing to provide time to deal with any unrepaired DNA damage that has occurred, thus preventing under-replicated DNA regions being taken beyond S-phase. CHK2 activity is necessary also for the activation of the G2/M cell cycle checkpoint, leading to an increase in phosphorylated CDK1 (the key effector of G2 checkpoint), thereby keeping it in its inactive state and delaying mitotic entry. The G2/M checkpoint really represents the last major opportunity for preventing DNA damage being taken into mitosis where unrepaired DSBs and under-replicated DNA may result in mitotic catastrophe and cell death (Bouwman and Jonkers, 2012; O'Connor, 2015; Pawlik and Keyomarsi, 2004).

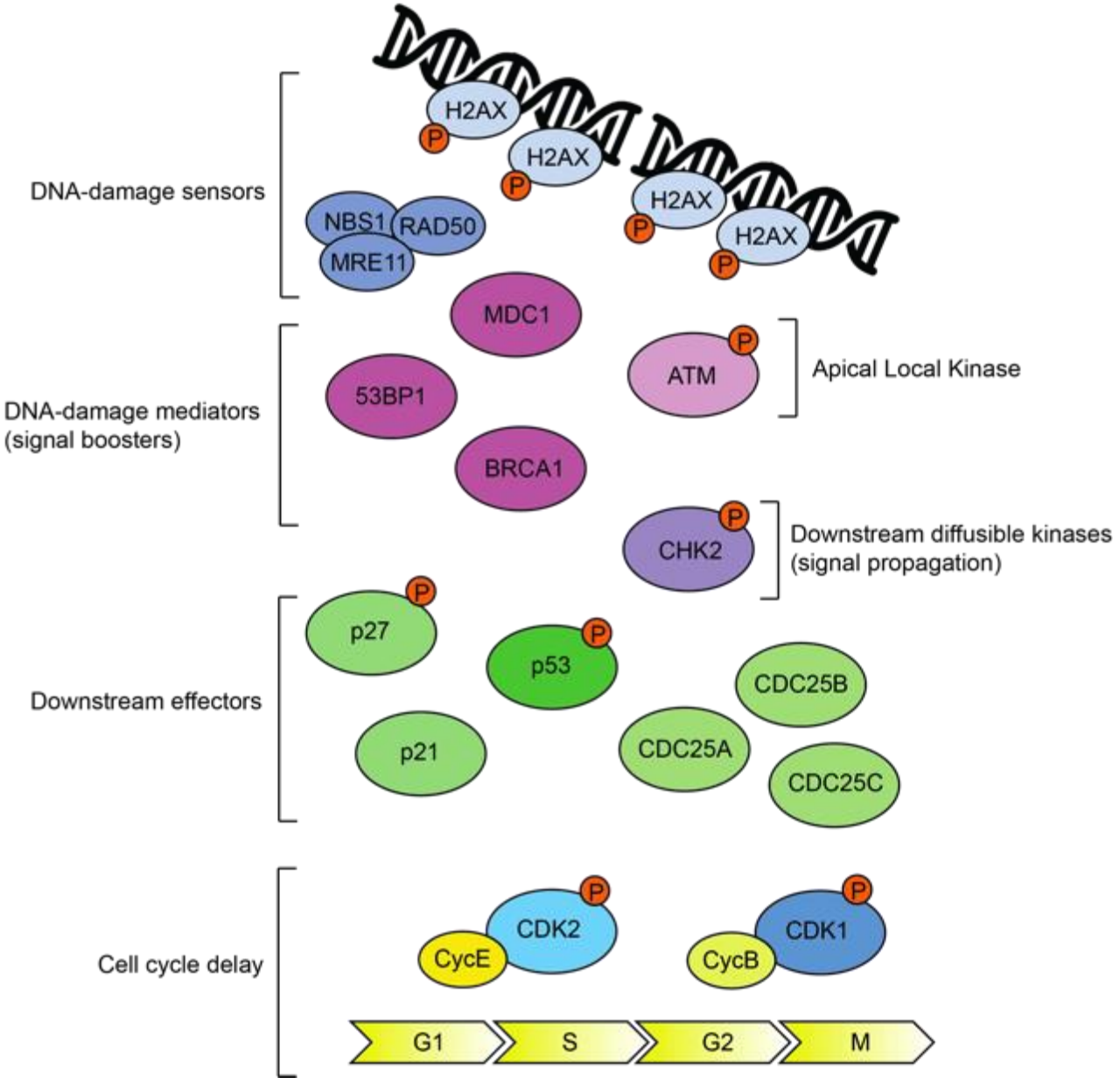

Figure 1. The DNA damage response to γ-radiation.

1.3.2.1.2 The γ-radiation therapy goal, schedules of treatment and side effects

The response to DNA damage is different depending on the cell-cycle status. DNA DSBs can be induced in all phases of the cell cycle, but their repair is likely to proceed optimally only in certain phases of the cell cycle, and alterations in chromatin conformation associated with cell cycle transitions may interfere with it. Damage registered during S phase can interfere with the functioning DNA replication machinery as well as lesions occurring in M phase alters mitosis process, both leading to serious genomic abnormalities (Iliakis et al., 2003). The biologic goal of γ-radiation treatment is to kill cancer cells

selectively without injuring normal tissues. Adult normal cells are generally in G0/G1 phase of cell cycle while the tumoral cells are more frequently in radiosensitive cell-cycle phases, such as mitosis.

Division of the γ-radiation dose into a number of treatment fractions provides two important biologic advantages: it allows DNA repair to take place within the normal tissues and allows proliferative tumor cells to redistribute through the cell cycle and move into the more radiosensitive phases (Buchholz, 2009). For this reason, most BC patients conventionally receive fractionated radiotherapy; typically consisting of 25 fractions of 2 Gy administered over 5 consecutive weeks. Recent studies collected the results of randomized trials of hypofractionated radiotherapy schedules that may change the current clinical practice. These retrospective data indicated that the use of hypofractionated radiotherapy in 13-16 fractions using 2.5-3.3 Gy per fractions to decreased total doses of 39-43 Gy administered within 3 weeks are as efficient and safe as conventionally fractionated radiotherapy for the majority of BC patients who need adjuvant radiotherapy after surgery (Budach et al., 2015; Speers and Pierce, 2016).

Radiotherapy remains an important treatment for the local control of BC, but unfortunately there are currently no robust and validated biomarkers for predicting its outcome. Not all patients derive therapeutic benefit since some BCs are refractory to this treatment, as evidenced by occurrence of distant metastatic spread and local recurrence. At present, decisions regarding who will receive radiotherapy and who will not are based on clinical factors, stages, morphology-based pathological indicators and type of surgery, rather than on molecular profiles predictive of likely radio-sensitivity. As a result, patients are currently treated with the same radiotherapy regimen, irrespective of whether their tumors are likely to respond or not (Langlands et al., 2013; Speers and Pierce, 2016).

Developing better biomarkers to identify patients at sufficiently low risk of recurrence such that adjuvant radiotherapy can safely be omitted or patients with radioresistant tumors is an important goal. A fortiori because radiotherapy it is not without risk of toxicity. The most common short-term subsequences to radiotherapy are skin erythema and fatigue. Following this, late side effects include telangiectasia (in the 31.4% of case) and impaired cosmetic with fibrosis (in the 6.7% of case). Over the last few decades, there has been an increased recognition of the late side effects of radiotherapy. Arm lymphedema and shoulder stiffness are other long-term side effects that can impact on patients' everyday activities. Post-operative breast radiotherapy can also damage the underlying chest organs, namely the lungs and heart. Pulmonary effects include γ-radiation induced

pneumonitis and fibrosis. Γ-radiation damage can also cause endothelial cell damage and atherosclerosis, myocardial ischemia and fibrosis. Complications such as acute pericarditis, pericardial effusion and arrhythmias, can also develop and, in some cases, can occur up to 20 years post treatment. The introduction of modern techniques (including image-based planning and directed therapies) has reduced γ-radiation doses to the heart and lungs. However, since some of the more severe late side effects of γ-radiations can occur many years following exposure, the full potential benefits of these changes is still uncertain (Langlands et al., 2013).

1.3.3 Endocrine therapy

Estrogen, a hormone produced by the ovaries, promotes the growth of ER+ BCs. Patients with ER+/PR+ breast tumor, like luminal ones, can be given endocrine therapy to block the effects of estrogen on the growth of BC cells. There are two main categories of endocrine therapy agents: aromatase inhibitors (AIs) and selective ER modulators (SERMs) (Miller et al., 2014).

AIs inhibit an enzyme called 'aromatase' that converts circulating testosterone to estradiol, and androstenedione to estrone, by aromatization. Such peripheral conversion of other hormones to estradiol is the main source of estrogen in postmenopausal women. Therefore, AIs only work when the primary source of estrogen is terminated either by the menopausal state, oophorectomy, or estrogen deprivation therapy using luteinizing hormone releasing hormone (LHRH) agonists. For this reason, AIs is the regimen of choice in post-menopausal patients. Exemestane, Anastrazole and Letrozole are the three main drugs of this category (Miller et al., 2014).

On the other hand, SERMs work in a completely different way. They competitively bind to ER to inhibit its proliferating stimuli. The three main drugs of this category are Tamoxifen, Raloxifen, and Toremifene (Miller et al., 2014). Adjuvant Tamoxifen is currently considered standard of care for pre- and post-menopausal women with endocrine-responsive disease. Five years of Tamoxifen have been shown to be effective in reducing the risk of recurrent disease and death in patients with ER+ BC. In particular, adjuvant Tamoxifen given for 5 years reduces by 31% the annual BC death rate of patients with ER+ disease (Colleoni and Munzone, 2015). However, the ATLAS (Adjuvant Tamoxifen: Longer Against Shorter) trial showed the benefit of longer Tamoxifen use. The extension of the treatment up to 10 years had a 4% improvement in BC related mortality. Based upon these data, the recent ASCO clinical guidelines indicated that after 5 years, women who are pre- or post-menopausal should be candidate to receive Tamoxifen for a total duration of 10 years, as

long as the patient can tolerate the treatment without side effects (Colleoni and Munzone, 2015; Miller et al., 2014).

Both luminal A and B tumors derive benefit from endocrine treatment, although the size of effect is larger in luminal A which usually receive only endocrine therapy (Ades et al., 2014; Goldhirsch et al., 2011). Respect the luminal A subtype, the luminal B is a more complex group, from both clinical and molecular points of view. For instance, although many of the luminal B tumors are ER+/HER2−/high Ki-67, expression profiles also classify the ER+/HER2+ tumors as luminal B and these patients receive a different therapy regimen (that incorporates targeted anti-HER2 therapy) compared to other luminal B BC subtypes (Bediaga et al., 2016). With respect to the HER2-negative luminal B tumors, they are inherently more aggressive, especially in the younger patients (Lee et al., 2015). Thus, one major challenge in the management of luminal B BC is to discriminate those patients that would benefit from cytotoxic drugs or anti-targeted therapy in combination with endocrine therapy from those that would not. As opposed to luminal A tumors, they should be treated with a more aggressive approach, which has not always demonstrated to be effective due to the molecular and clinical heterogeneity of this BC subtype (Bediaga et al., 2016).

1.3.3.1 Overcoming endocrine resistance in Luminal breast cancer

Given that luminal B BC appear to rely less on the estrogen pathway and that metastatic LBC could develop *de novo* or acquired resistance to endocrine therapy, clinical trial studies have considered targeting alternative pathways (Ades et al., 2014; Creighton, 2012). Figure 2 shows an overview of the signaling pathways under blockade with targeted compounds in LBCs: PI3K/AKT/mTOR, FGFR1 (Fibroblast growth factor 1 receptor), IGFR1 (insulin-like growth factor 1 receptor), CDK4/6 inhibitors activity.

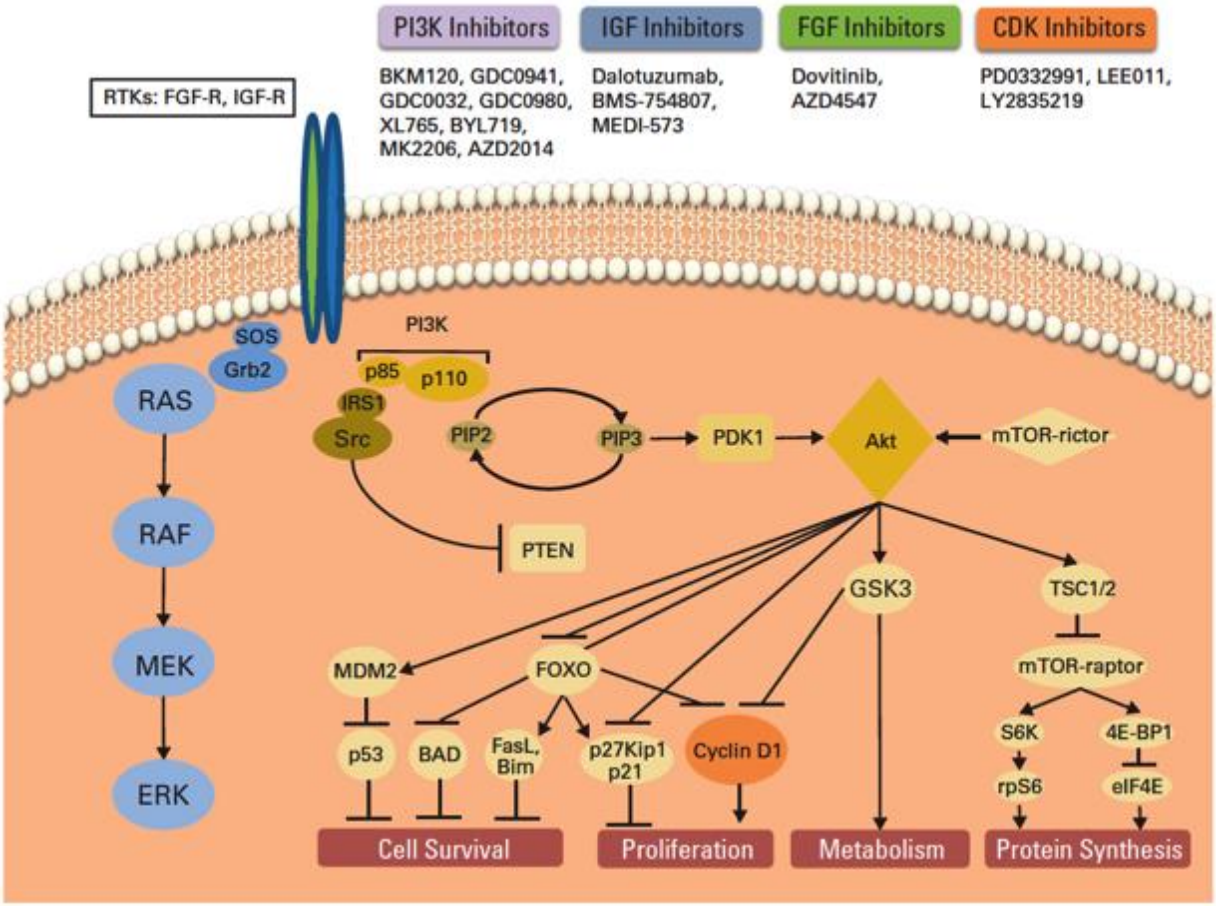

Figure 2. Signaling pathways under blockade with target compounds in LBC (Ades et al., 2014).

Compounds for FGFR1 and IGF1R pathways inhibition are in study. FGFR1 amplification has been associated with high proliferative tumors, up to 27% of luminal B tumors, and with poor prognosis. IGF1R signaling pathway causes activation of the PI3K/AKT/mTOR and Ras/Raf/MEK/ERK pathways. In LBC, there is IGF1R-ER crosstalk, where ER up regulates IGF1R, and IGFR1 signaling boosts the proliferative effect of estrogen (Ades et al., 2014). The only two targeted agents currently approved by the FDA to treat ER+/HER2- BC, reported by the National Comprehensive Cancer Network, are the mTOR inhibitor Everolimus and the CDK4/6 inhibitor Palbociclib (Gu et al., 2016).

The most promising results for targeting the crosstalk between ER and the PI3K/AKT/mTOR pathway have come from combining Everolimus with endocrine therapy in patients with metastatic BC in the BOLERO II phase III clinical trial, but it remains to be shown whether the strategy of combining PIK3 blocking with endocrine therapy will improve early stage BC clinical outcome (Ades et al., 2014; Ignatiadis and Sotiriou, 2013).

1.3.3.2 Targeting cell cycle in luminal breast cancer

The mitotic cell cycle is a tightly regulated universal process that ensures the correct division of one cell into two daughter cells and that underlies the growth and development of all living organisms (Nurse, 2000). The division consists in four discrete phases: the DNA synthesis and duplication phase (S phase); the mitosis (M phase), which consist in generation of bipolar spindles, segregation of sister chromatids and cytokinesis to form two daughter cells; the gap phases that take place between the M and S phase and between S and M phase, called gap phase 1 (G1) and 2 (G2), respectively. The G1 is the interval between the M and the S phase. During the G1 phase, the cell integrates the mitogenic and inhibitory signals and make the decision to proceed, pause or exit the cell cycle. The term G0 is used to describe cells that have exited the cell cycle and become quiescent (Israels, 2000). During the G2 phase, mechanisms that ensure that the DNA has been faithfully replicated take place and permit the subsequent start of M phase.

To ensure proper progression through the cell cycle, cells have developed a series of checkpoints that prevent them from entering into a new phase until they have successfully completed the previous one (Hartwell and Weinert, 1989). The progression along the different phases of cell cycle is positively regulated by the sequential activation of the so-called cyclin dependent kinases (CDKs), evolutionary conserved serine-threonine kinases. CDKs are activated along the different phases by associating with their regulatory partner member of the cyclin family. Their activity is counteracted by small proteins known as CDK inhibitors (CKIs). Two different families of CKIs exist, the INK4 and the Cip/Kip proteins. The INK4 (Inhibitors of CDK4) family includes $p16^{INK4a}$, $p15^{INK4b}$, $p18^{INK4c}$ and $p19^{INK4d}$. All these members exert their inhibitory activity by binding to the CDK4 and CDK6 kinases and preventing their association with D-type cyclins. INK4 members are responsible for G1 cell cycle arrest and can block proliferation only through a functional RB pathway. The Cip/Kip family includes $p21^{Cip1}$, $p27^{Kip1}$ and $p57^{Kip2}$, all characterized by the presence of a conserved N-terminal region containing the cyclin-CDK binding domain, whereby they interact with the regulatory and catalytic subunit of every complex (Belletti et al., 2005).

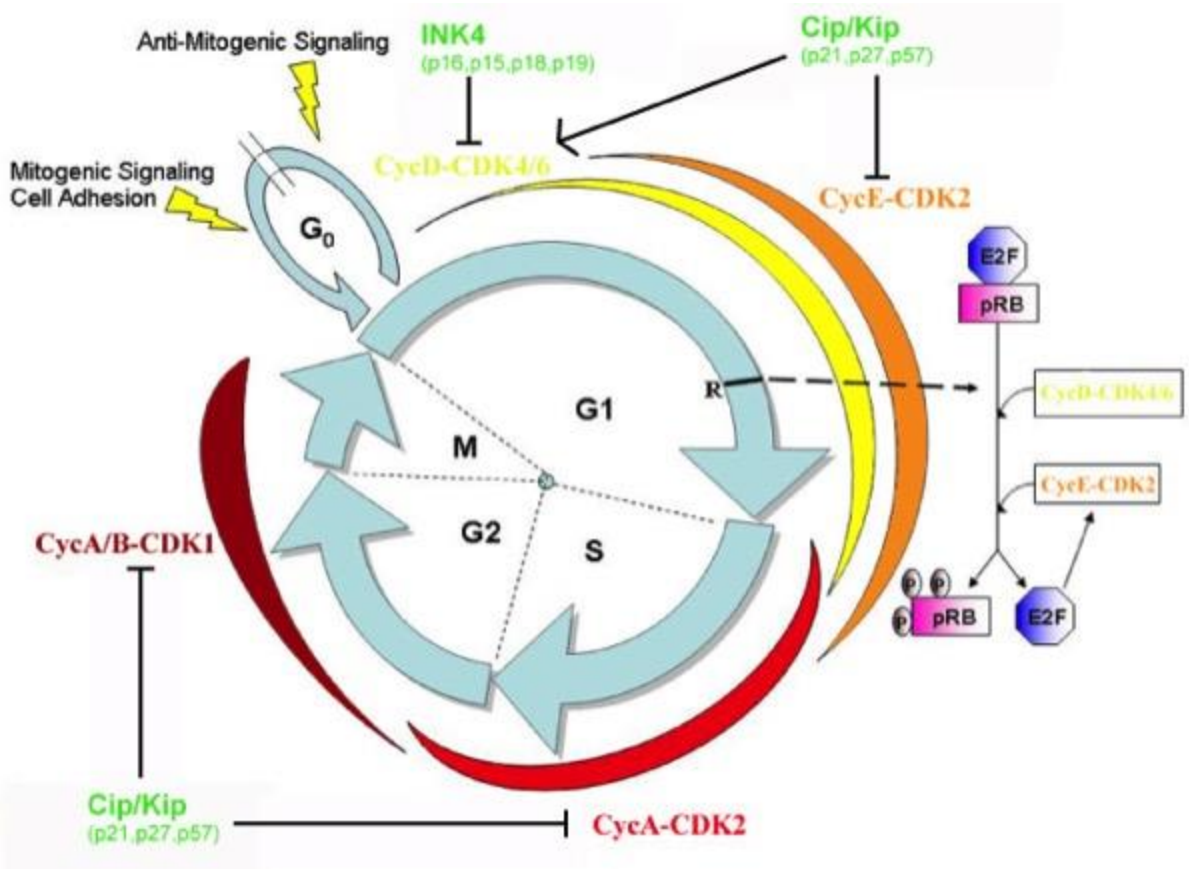

Figure 3. Schematic representation of cell cycle regulation. The passage through the R point is due to the inactivation of the pRB protein by CDKs-dependent phosphorylation (Belletti et al., 2005).

Retinoblastoma (RB) captures a key function in cell cycle control. Under normal conditions the unphosphorylated RB is bound to members of the transcription factor family E2F, which in turn are linked to a protein called dimerization partner (DB). Mitogenic signals stimulate the expression of cyclin D, which activates the CDK4 and CDK6, resulting in the phosphorylation of RB. Thereby RB disassociates from E2F allowing the transcription of E2F-dependent genes. Cyclin E/CDK2 or cyclin A/CDK2, cyclin A/CDK1 or cyclin B/CDK1 augment this phosphorylation process. E2F induces the expression of cell cycle genes, including cyclins and CDKs, and of genes involved in replication and mitosis enabling progression from G1-phase to S-phase and to mitosis. At the transition from M- to G1-phase, RB is dephosphorylated and thereby activated again by phosphatases (Gampenrieder et al., 2016).

Amplification of both cyclin D1 and CDK4 is especially high in luminal B (58 % and 25 %, respectively) and intermediate in luminal A (29 % and 14 %, respectively) (Koboldt et al., 2012). Such alteration of cell cycle elements is associated with worse prognosis in ER+ BC and is a known mechanism of endocrine resistance. Consequently, CDK4/6 inhibition seems a reasonable target for LBC treatment. Preclinical data show that the sensitivity to CDK4/6 inhibition is restricted to luminal and HER2-amplified BC cell lines, while non-

luminal cell lines harbor intrinsic resistance. Synergistic effect of CDK4/6 inhibitors and endocrine therapy has been widely shown in preclinical models (Gampenrieder, Rinnerthaler, and Greil 2016). Finn et al. examined the effects of Palbociclib (or PD0332991, one of the CDK4/6 inhibitors synthetized) in 47 human breast cancer cell lines, alone and in combination with Tamoxifen. They found that ER+ cell lines were the most sensitive to growth inhibition by the drug, displaying G0/G1 arrest and decreased Rb phosphorylation in response to Palbociclib. They also found that Palbociclib and Tamoxifen were synergistic in ER+ cells lines (Finn et al., 2009; Gampenrieder et al., 2016; Wardell et al., 2015). These observations have been recently followed by a phase I/II clinical study that has now demonstrated significant clinical activity in patients with advanced ER+ BC. For these reasons, now Palbociclib in combination with the aromatase antagonist Letrozole is FDA-approved for the treatment of post-menopausal women with ER+/HER2− advanced BC and as first-line endocrine-based therapy for metastatic disease (Roskoski 2016; Finn et al. 2015).

1.4 p27^{Kip1}

p27^{Kip1} is well known to be a tumor suppressor gene. But, while prototypic tumor suppressor genes follow the Knudson's "two-hit" theory, p27^{Kip1} is haplo-insufficient for tumor suppression. Animals lacking one copy of CDKN1B gene (codifying for p27^{Kip1}) develop tumors spontaneously late in life and are highly sensitive to tumor induction when challenged with carcinogens, displaying increased tumor frequency and decreased latency (Fero et al., 1998). p27^{Kip1}-/- mice display increased body size of about 20-30% respect to wild-type (WT) littermates, due to increased cellularity of tissues, demonstrating a role of p27^{Kip1} in the control of tissue growth also *in vivo*. Further, p27^{Kip1} Knock-Out (KO) mice are prone to spontaneous pituitary adenomas and develop multiple organ hyperplasia (Fero et al., 1998; Nakayama et al., 1996).

An increased body of literature reports frequent p27^{Kip1} functional inactivation in human cancers. The completely loss of p27^{Kip1} is not uncommon in human malignancies, but silencing or mutations of both alleles are very rare, which is consistent with the notion that p27^{Kip1} loss in tumors is mainly due to an accelerated proteolysis. Accordingly, a plethora of studies shows the involvement of p27^{Kip1} protein reduction or loss in many tumors, such as carcinomas of the colon, breast, prostate, lung and ovary as well as brain tumors, lymphomas and soft tissue sarcomas (Belletti et al., 2005).

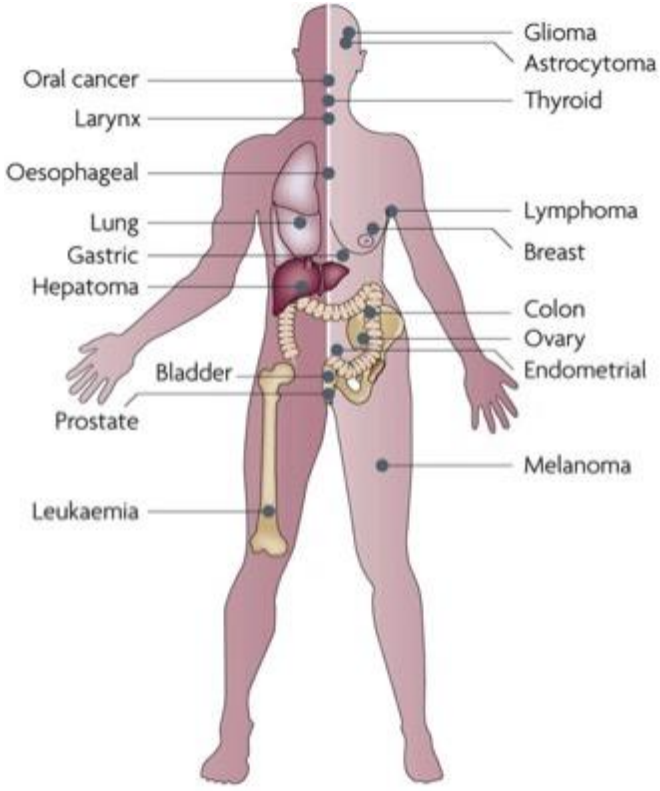

Figure 4. The majority of human malignancies in many organ sites that show reduced p27^{Kip1} protein levels (Chu et al., 2008).

Regarding BC, in a retrospective analysis of $p27^{Kip1}$ in 2,031 cancer samples from a randomized clinical trial, reduced $p27^{Kip1}$ was an independent prognostic factor for reduced overall survival (Porter et al., 2006). In another work, in 500 patients with premenopausal ER+ BC low $p27^{Kip1}$ correlated strongly with poor survival, showing the predictive potential of $p27^{Kip1}$ in a prospective trial (Pohl, 2003). Through meta-analysis of 20 studies, Guan *et al.* correlate $p27^{Kip1}$ expression and clinical outcome of BC including overall survival (OS), disease-free survival (DFS) and relapse-free survival (RFS). A total of 60% of the studies showed a significant association between $p27^{Kip1}$ high expression and OS, whereas 25% and 60% studies demonstrated a correlation between $p27^{Kip1}$ high expression and DFS and RFS, respectively (Guan et al., 2010). Together, these data indicates that reduced $p27^{Kip1}$ is an independent prognostic factor for poor OS and DFS. Moreover, reduced $p27^{Kip1}$ correlates with lower cyclin D1 (Barnes et al., 2003; Gillett et al., 1999) and with *ERBB2* (the gene encoding for HER2) amplification (Newman et al., 2001; Spataro et al., 2003). Recent whole genome sequences data suggest that CDKN1B is frequently mutated in some types of human cancer, including LBC. Mutations of CDKN1B in LBC occur, in more than half of the cases, in the C-terminal portion of the protein, suggesting that tumor suppressive activities are present in this region (Belletti and Baldassarre, 2012; Koboldt et al., 2012; Stephens et al., 2012).

1.4.1 $p27^{Kip1}$ during the cell cycle

Among the CDK inhibitors, $p27^{Kip1}$ is well known for its role during G1/S phase transition of the cell cycle. It interacts with and inhibits cyclinE-CDK2 and cyclinA-CDK2 activity, thereby blocking cell cycle progression. The crystal structure of the human $p27^{Kip1}$ bound to the phosphorylated cyclinA-CDK2 complex revealed that $p27^{Kip1}$ binds the complex as an extended structure interacting with both cyclin A and CDK2. On cyclin A, it binds in a groove formed by conserved cyclin box residues. On CDK2, it binds and rearranges the amino-terminal lobe and also inserts into the catalytic cleft, mimicking the ATP (Russo et al., 1996). In early G1, $p27^{Kip1}$ promotes cyclin D-CDK4/6 complex assembly and nuclear import, increasing cyclin D stability, all without inhibiting CDK4 kinase activity. In proliferating cell, $p27^{Kip1}$ is primarily associated with cyclin D-CDK4/6 complexes, but these complexes are catalytically active, whereas in G1 arrested cells $p27^{Kip1}$ preferentially binds and inhibits cyclin E-CDK2. The sequestration of $p27^{Kip1}$ by cyclin D-CDK4/6 complexes effectively frees CDK2 from inhibition and allows both CDK4/6 and CDK2 to remain active. In this way, mitogen induction of cyclin D expression determines cell cycle progression

both activating CDK4 and by sequestering $p27^{Kip1}$, thus eventually favoring cyclin E-CDK2 activation. Once CDK2 becomes active, it triggers the degradation of $p27^{Kip1}$ by phosphorylating it on a specific threonine residue (Thr-187) (Sherr and Roberts, 1999), thus reinforcing CDK4 activity to complete Rb phosphorylation.

Several works on $p27^{Kip1}$ regulation during cell cycle progression have revealed a role for $p27^{Kip1}$ also in G2/M transition. Historically $p27^{Kip1}$ was discovered as a universal inhibitor of CDKs, able to bind *in vitro* also cyclin E/A- CDK1 complexes, whose kinase activity is crucial for mitosis entry (Toyoshima and Hunter, 1994). Nakayama and colleagues have demonstrated *in vivo* how $p27^{Kip1}$ accumulation at G2/M transition induces a strong decrease in CDK1 associated activity (Nakayama et al., 2004). The prolonged G2 arrest induced by $p27^{Kip1}$, through the suppression of CDK1 activity, was shown to be responsible for centrosome duplication, cell endoreplication (increase in cell genomic content without an associated cell division) and cell polyploidy (Serres et al., 2012; Sharma et al., 2012).

$p27^{Kip1}$ gene, CDKN1B, resides in a region of chromosome 12p13 and encodes for a 198 aminoacids protein, with distinct domains (Figure 5). From the residue 153 to 169 is present a nuclear localization signals, while a leucine rich nuclear export signal, responsible for $p27^{Kip1}$ shuttling from nucleus to cytoplasm, is localized between aminoacids 32-46. The cyclins/CDKs-binding domains reside instead between the 25-32 aminoacids and between the 46-93 aminoacids, respectively.

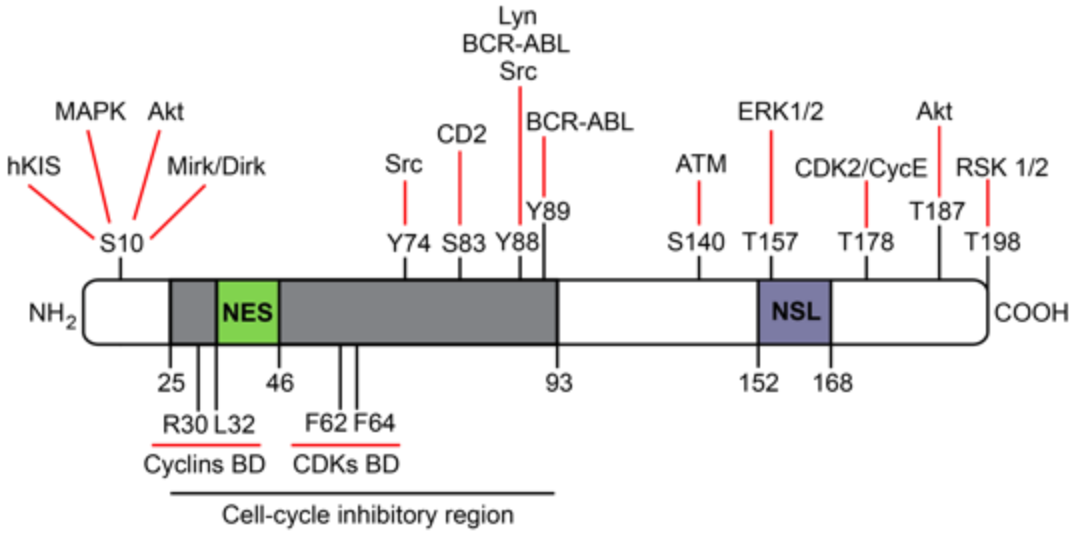

Figure 5. $p27^{Kip1}$ structure with principal domains and phosphorable sites.

The abundance of $p27^{Kip1}$ within the cell is controlled by multiple mechanisms that operate at level of its synthesis (transcription/translation) and, particularly, its stability, degradation and localization. In fact, although mRNA levels are usually constant through out the whole

cell cycle, $p27^{Kip1}$ expression in normal cells is finely regulated and high levels of the protein induce the arrest in G1 phase and cell accumulation in G0. $p27^{Kip1}$ levels increase in response to various stimuli that inhibit cell proliferation, such as cell-cell contact, loss of adhesion to extracellular matrix, stimuli inducing cell differentiation or TGFβ (Transforming growth factor β) , INF-γ (Interferon-γ), c-AMP, rapamicin and lovastatin treatments (Belletti et al., 2005). The exit from the quiescent status requires the down-regulation of $p27^{Kip1}$, which in turn results in CDKs activation. $p27^{Kip1}$ can also be regulated by sequestering into higher order complexes with cyclin D-CDK4 (as described hereafter) after activation of the MAPK pathway, that promotes cyclin D transcription (Susaki and Nakayama, 2007). Also the proto-oncogene c-Myc, by increasing the expression of cyclin D and cyclin E, is responsible for $p27^{Kip1}$ sequestration and this molecular event appears essential for Myc-induced cell cycle progression (Vlach et al., 1996). Moreover, $p27^{Kip1}$ can be displaced in the cytoplasm, with consequent progression in cell cycle, after phosphorylation of Serine 10 by KIS (kinase-interacting Stathmin) or by MAPK and/or phosphorylation of Threonine 198 by Akt or RSK (Belletti et al., 2005; Philipp-Staheli et al., 2001).

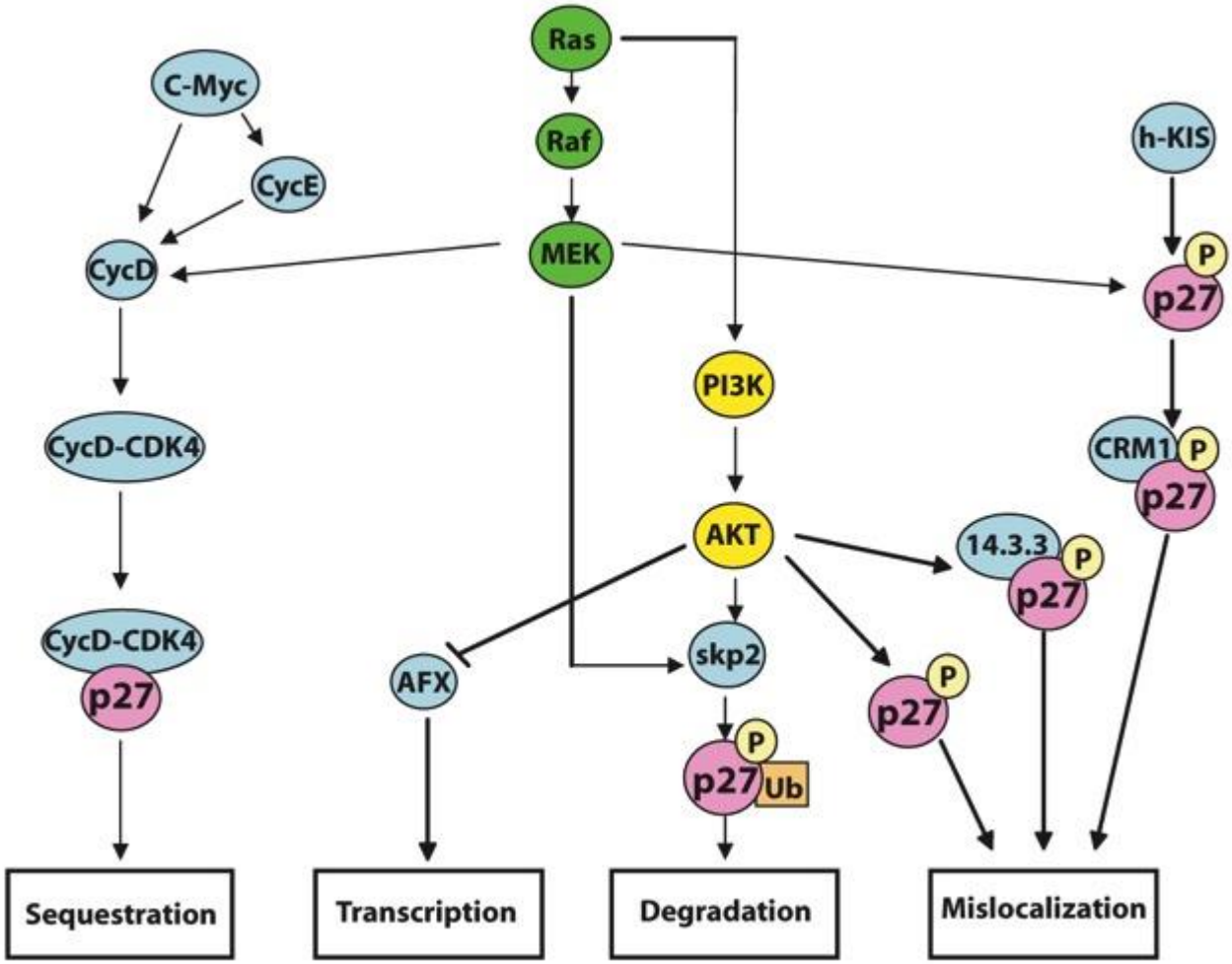

Figure 6. Representation of the different intracellular pathways known to regulate p27 expression and function (Belletti et al., 2005).

The translocation of $p27^{Kip1}$ from the nucleus to the cytoplasm is followed by its degradation by the ubiquitin-proteasome pathway by the KPC complex (Kip1 ubiquitination-promoting complex), consisting of KPC1 and KPC2 proteins, that interacts with and ubiquitinates $p27^{Kip1}$ in the cytoplasm (Kamura et al., 2004; Kotoshiba et al., 2005). The nuclear export of $p27^{Kip1}$ by CRM1 is necessary for KPC-mediated proteolysis and the recognition by CRM1 needs $p27^{Kip1}$ phosphorylation on Ser10 (Boehm et al., 2002; Kamura et al., 2004). $p27^{Kip1}$ proteolysis is cytoplasmatic and KPC-dependent in early G1, but it is nuclear in late S/G2 phase. In S/G2 phase, degradation is mediated by an SCF ubiquitin ligase, composed by Skp1, a cullin subunit called CulI, Rbx1/Roc1 and the F-box protein Skp2 that specifically recognizes $p27^{Kip1}$. Skp2 binds to $p27^{Kip1}$ and promotes its degradation when $p27^{Kip1}$ is phosphorylated on the conserved Thr187 by cyclinE-CDK2 or cyclinA-CDK2 complexes (Hara et al., 2001).

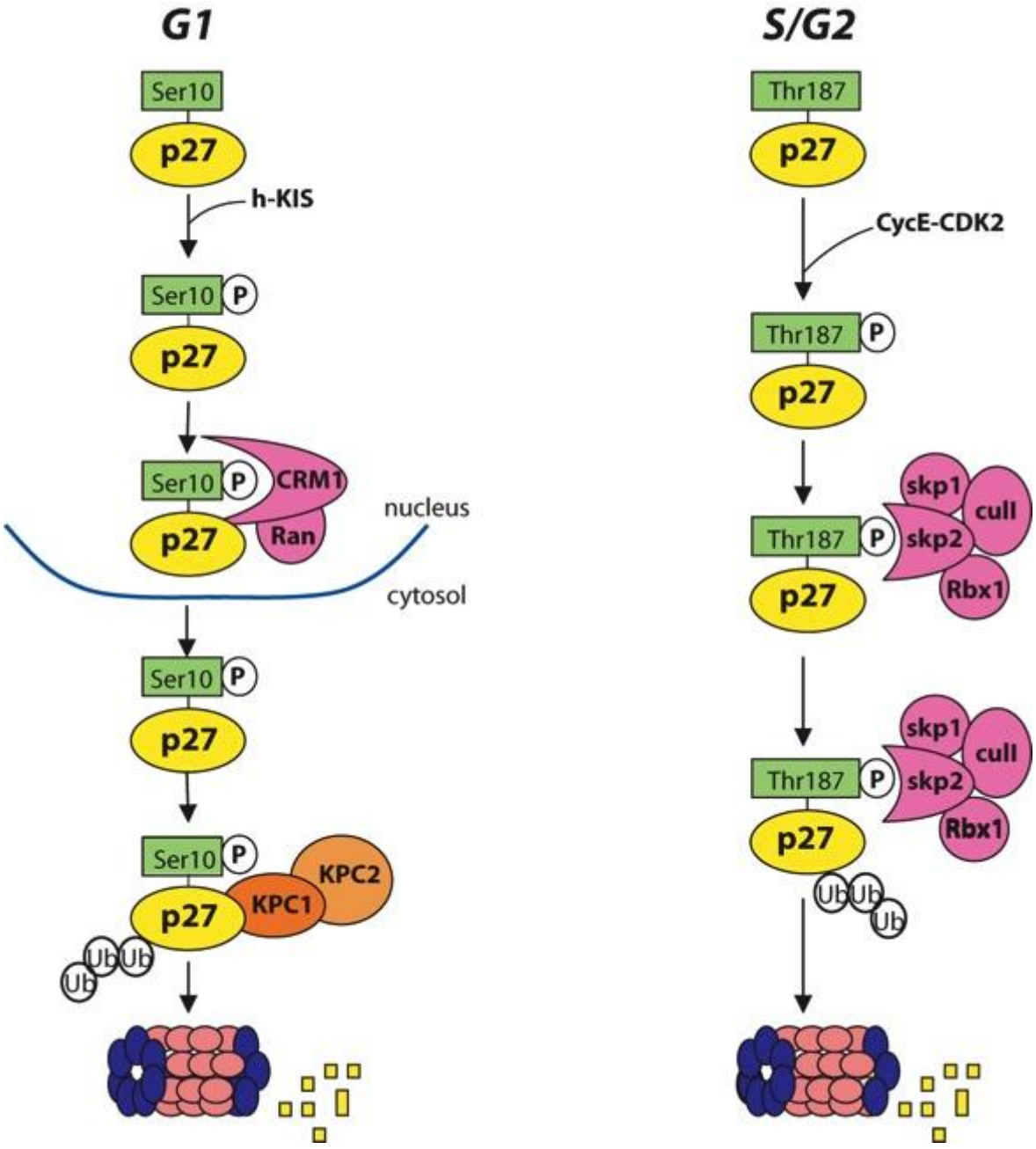

Figure 7. Mechanisms regulating p27^{Kip1} ubiquitin-dependent degradation during cell cycle (Belletti et al., 2005)

Several distinct kinases determine p27^{Kip1} phosphorylation status during cell cycle. The phosphorylation at Ser10 plays a critical role to decrease p27^{Kip1} nuclear abundance below a certain threshold, thereby allowing for the initial activation of cyclin-CDKs complexes (Besson, 2006; Ishida et al., 2000; Rodier et al., 2001). This serine is a substrate for at least four enzymes, after mitogenic stimuli. These include human Kinase Interacting with Stathmin (hKIS) (Boehm et al., 2002; Vervoorts and Lüscher, 2008), MAPK (Rodier et al., 2001), Akt/PKB (Vervoorts and Lüscher, 2008) and Mirk/Dirk1B (Besson, 2006). The T187 of p27^{Kip1} is phosphorylated by the cyclin E-CDK2 and cyclinB-CDK1 (Sheaff et al., 1997;

Vlach, 1997), and leads to its degradation *via* the ubiquitin-proteasome system (Grimmler et al., 2007; Hara et al., 2001). Under high glucose stimulation, MAP kinases ERK1/2 have been reported to phosphorylate $p27^{Kip1}$ at S10, T187 and S178 in mesangial cells, both *in vitro* and *in vivo* (Wolf et al., 2003). Other important phosphorylation sites of $p27^{Kip1}$ are the T157 and the T198, both regulated by AKT. The T157 residue maps within the nuclear localization signal of $p27^{Kip1}$ and the AKT-mediated T157 phosphorylation causes retention of $p27^{Kip1}$ in the cytoplasm, precluding $p27^{Kip1}$-induced G1 arrest (Liang et al., 2002; Shin et al., 2002; Viglietto et al., 2002). AKT phosphorylates $p27^{Kip1}$ also at T198. Once phosphorylated on this residue, $p27^{Kip1}$ is recognized by the 14-3-3 family of proteins and retained in the cytoplasm (Fujita, 2002). It has been demonstrated that phosphorylation at T198 is able to regulate $p27^{Kip1}$ stability, localization and interaction with Stathmin, interfering with $p27^{Kip1}$ ubiquitination and $p27^{Kip1}$ role in cell motility (Schiappacassi et al., 2011). The tyrosines Y74, Y88 and Y89, located in the CDK-binding domain, are phosphorylated preferentially in proliferating cells, converting $p27^{Kip1}$ to a non-inhibitory state (James et al., 2008). Grimmler and colleagues have reported that the residue Y88 can be phosphorylated by the Src-family kinase Lyn and by the oncogene product BCR-ABL. Once phosphorylated on Y88, $p27^{Kip1}$ is also efficiently phosphorylated on T187 by CDK2 and in turn its SCF-Skp2-dependent degradation is promoted, suggesting an explanation for premature $p27^{Kip1}$ elimination in cells transformed by these activated tyrosine kinases (Grimmler et al., 2007). The oncogenic kinase Src regulates $p27^{Kip1}$ stability through its phosphorylation not only at Y88 but also at tyrosine 74 and, to a less degree, at tyrosine 89. Also in this case, the phosphorylation facilitates $p27^{Kip1}$ proteolysis (Chu et al., 2007). Between these tyrosine residues, $p27^{Kip1}$ could be phosphorylated at serine 83 by CK2 (Tapia et al., 2004) in cardiomyocites stimulated by angiotensin II, a major cardiac growth factor, inducing its proteasomal degradation (Hauck et al., 2008). Recently, it has been shown that serine in position 140 can be phosphorylated by ATM kinase after DNA damage induced by ionizing γ-radiation, stabilizing $p27^{Kip1}$ for G1/S cell cycle checkpoint activation (Cassimere et al., 2016).

1.4.2 $p27^{Kip1}$, DNA damage and genomic stability.

The maintenance of genomic integrity is a fundamental hallmark in cell biology. Given the potentially devastating effects of the genomic instability, cells have developed a complex series of mechanisms to maintain and preserve the gene pool (Lord and Ashworth, 2012). As previously described, after lesion to the DNA, the responsive pathway is responsible to delay and/or avoid proliferation of damaged cells and the consequent propagation of

genetic defects, maintaining cells genomic stability. $p27^{Kip1}$ is one of the molecular player that is involved in DDR pathway (Cuadrado et al., 2009).

The generation of $p27^{Kip1}$ KO mouse model provided a useful system to study the effects of $p27^{Kip1}$. Besides alterations related to proliferative dysfunctions, such as the increase in the body size due to a general tissue hypercellularity and the development of spontaneous pituitary adenomas, $p27^{Kip1}$-deficient mice show a higher susceptibility to genotoxic- and γ-radiation-induced tumors (ENU, DMH and γ-radiation) with a decreased tumor free survival, higher tumor mortality and higher number of tumors *per* mouse, suggesting a role of $p27^{Kip1}$ in the control of genomic stability (Fero et al., 1998). More specifically, after γ-radiations, $p27^{Kip1}$ deficiency has been associated to higher micronucleus frequency in reticulocyte preparations and to chromatid breaks in spleen cultures (Payne et al., 2008).

It has been also suggested that an accumulation of $p27^{Kip1}$ after DNA damage is required to suppress centrosome amplification, thereby preventing chromosomal instability (Sugihara, 2006). Sharma and colleagues investigated the role of $p27^{Kip1}$ in the control of centrosome amplification by expressing different mutants of $p27^{Kip1}$ in human osteosarcoma cell lines (U2OS). The authors demonstrated that the expression of $p27^{Kip1}$K, a mutant with a defective CDK-binding site and, consequently, not able to inhibit cell cycle progression, is associated with the presence of more than two centrosomes in the cells, with mitotic catastrophe and multiple micronuclei in standard growing conditions (Sharma et al., 2012). Mice expressing a form of $p27^{Kip1}$ that is unable to bind or inhibit cyclin-CDK complexes ($p27^{Kip1}$CK–) presents a phenotype of multinucleation and polyploidy. Serres and colleagues suggested that this form of $p27^{Kip1}$ is not able to interact with the Rho effector citron kinase (citron-K) co-localizing at the contractile ring and mid-body (Serres et al., 2012).

In mouse gastrointestinal tumors induced by genotoxic carcinogens and γ-radiations, $p27^{Kip1}$ deficiency resulted in an increased mitotic index, small/large scale genetic lesions and higher mutation frequency, effects that can be due, at least in part, to an inefficient G2/M checkpoint activation (Payne et al., 2008). One possible explanation is that, following cell γ-radiation, the G2/M checkpoint needs to be quickly activated to prevent that damaged DNA is inherited by daughter cells and G2/M checkpoint activation and resolution relay on the inhibition of CDK1 activity (Deckbar et al., 2011), which is target of $p27^{Kip1}$ (Nakayama et al., 2004). Moreover, p38 MAPK-dependent stabilization of $p27^{Kip1}$ was shown to be essential for a G2/M checkpoint arrest in response to prolonged exposure to DNA breaks (Cuadrado et al., 2009). Though the molecular mechanisms by

which $p27^{Kip1}$ regulates genomic integrity are not very well understood, recent study proved that $p27^{Kip1}$ is essential for the establishment of the G1 cell cycle checkpoint arrest preventing cells from entering S-phase after DNA damage. Cassimere and colleagues found that ATM kinase directly phosphorylates $p27^{Kip1}$ at residue S140, thereby increasing its half-life in a rapid and transient manner after the induction of DNA DSBs with genotoxic agents (Cassimere et al., 2016).

In the light of $p27^{Kip1}$ possible involvement in genomic stability and DDR pathway, $p27^{Kip1}$ could have a potential predictive role for γ-radiation responsiveness. In support of this, two different studies in the field of esophageal carcinoma cells showed a direct correlation between $p27^{Kip1}$ expression and radioresistance. Wang and colleagues proved a negative correlation between high SKP2, a protein that forms a stable complex with cyclin A/CDK2 and specifically recognizes and promotes the degradation of $p27^{Kip1}$, expression and the survival of patients with esophageal squamous cell carcinoma who received radiotherapy (Wang et al., 2012). The other study, from Tong and colleagues, showed that there's a change in cell cycle phase distribution in esophageal carcinoma cells being radioresistant: after repeated γ-radiation, these cells presented a percentage of S phase cells significantly increased and a $p27^{kip1}$ expression lower than that of parental cells (Tong et al., 2011).

1.4.3 $p27^{Kip1}$ in the endocrine therapy for breast cancer.

In vitro, it has been proved that $p27^{Kip1}$ is required for G1 arrest by Tamoxifen or estrogen deprivation, in ER+ BC lines (Cariou et al., 2000). In clinic, various important studies of $p27^{Kip1}$ in randomized trial populations suggest that high $p27^{Kip1}$ may predict response to endocrine therapy. Porter and colleagues analyzed 2,031 patients from the South Western Oncology Group (SWOG) S9313 trial who were randomized to receive adjuvant doxycycline and cyclophosphamide, with adjuvant Tamoxifen given for ER+ cancers. They found that $p27^{Kip1}$ was a stronger independent prognostic factor in ER+ tumors than in the entire group (Porter et al., 2006). In another trial that randomized 512 premenopausal women with ER+ positive cancers to receive either Tamoxifen with ovarian suppression or chemotherapy with no subsequent endocrine therapy, reduced $p27^{Kip1}$ expression was strongly predictive of failure of adjuvant hormonal therapy (Pohl, 2003). Huh *et al.* investigated the association between BC risk and the frequency of mammary epithelial cells expressing $p27^{Kip1}$, ER and Ki67 in normal breast tissue. Performing a nested case-control study of 302 women who had been initially diagnosed with benign breast disease, they highlighted that high Ki67+/low $p27^{Kip1}$+ and high Ki67+/low ER+ cell frequencies were significantly associated with a 5-fold higher risk of BC compared with low Ki67+/low

$p27^{Kip1}$+ and low Ki67+/low ER+ cell frequencies, respectively, among premenopausal women (Huh et al., 2016). Taken together, data from these studies support the idea that $p27^{Kip1}$ could have a predictive role for the response to Tamoxifen and to other antiestrogen treatments (Chu et al., 2008).

1.4.4 $p27^{Kip1}$ and cell motility.

Regulation of cell motility requires the cytoplasmic localization of $p27^{Kip1}$, so results dependent on all those mechanisms that rule $p27^{Kip1}$ shuttling from nucleus to cytoplasm. Many authors have demonstrated a role of $p27^{Kip1}$ in cell migration, but the conclusions are at least apparently in contrast. It was shown that $p27^{Kip1}$ stimulates the migration in cortical neurons and in hepatocellular carcinoma cells, where it induces rearrangements of the actin cytoskeleton (Besson, 2004; Itoh et al., 2007; Kawauchi, 2015; McAllister et al., 2003). Conversely, $p27^{Kip1}$ seems to reduce cell migration in endothelial cells, vascular smooth muscle cells, mesangial cells, sarcoma tumor cells and normal mouse fibroblasts (Baldassarre et al., 2005; Daniel et al., 2004; Goukassian, 2001; Sun et al., 2001).

Stathmin is a protein that binds to $p27^{Kip1}$ C-terminus to coordinate cell motility. Stathmin, also referred to as Op18, is a ubiquitous cytosolic phosphoprotein (Maucuer et al., 1993). This 149 aminoacids protein plays an important role in regulating microtubule dynamics in both interphase and mitotic cells and it is crucial for the maintenance of cell shape, intracellular transport, cell motility and division. Microtubules continuously switch between phases of polymerization and depolymerization, a property known as dynamic instability. Stathmin is a microtubule-destabilizing protein that promotes microtubule depolymerization by two distinct mechanisms. The first is a catastrophe-promoting microtubule-depolymerization activity that requires the N-terminal region of the protein and is necessary for the regulation of the mitotic spindle. The second is a tubulin-sequestering activity that requires the C-terminal region and is important in mainly the regulation of microtubule dynamics during interphase (Rubin and Atweh, 2004). $p27^{Kip1}$ binds the C-terminus of Stathmin, thus mainly interfering with its ability to sequester free tubulin heterodimers, leading to increased microtubule stabilization. In the absence of $p27^{Kip1}$, an increased MT-destabilization could, in turn, be responsible for increasing the migration of the cell (Baldassarre et al., 2005; Schiappacassi et al., 2011), altering the morphology and ability to invade in cells immersed in three-dimensional (3D)-matrices (Belletti et al., 2008, 2010).

1.4.5 $p27^{Kip1}$ and stemness.

An active role of $p27^{Kip1}$ in the differentiation process has been mainly deduced by the evidence that its expression increases in most terminally differentiated cells. Initially, it was thought that $p27^{Kip1}$ was only responsible to arrest cells in G1 prior to the stage of differentiation, but now it is certain that his role is far more sophisticated.

In some cell lines like NT2/D1, the constituvely expression of $p27^{Kip1}$ not only stops cells proliferation but also promotes the differentiation (Baldassarre et al., 1999). Recently, it has been shown that overexpression of $p27^{Kip1}$ in mouse pluripotent stem cells (miPSCs) preserves their pluripotency characteristics but induces the loss of the stemness-state earlier than in normal miPSCs during embryoid body and teratoma formation in a mouse model of coronary artery ligation (Matsu-ura et al., 2016).

$p27^{Kip1}$ was also documented as an intrinsic “timer” during the proliferation of cardiomyocytes (Burton et al., 1999) and oligodentricyte, *in vitro* (Gao et al., 1997). Using $p27^{Kip1}$ KO mice in conjunction with the hematopoietic reconstitution assay, it has been reported that the loss of $p27^{Kip1}$ hasn’t an effect on the hematopoietic cells self-renewal, but markedly alters their proliferation and pool size (Cheng, 2000).

Nguyen et al. demonstrated that $p27^{Kip1}$ is able to induce neuronal differentiation and that this activity is a cell cycle-independent function. In fact, the mutant $p27^{Kip1}$ CK- used in this investigation remains able to promote the expression of neuronal differentiated markers, still remaining unable to bind cyclins and CDKs (Nguyen, 2006; Nguyen et al., 2006). Li and colleagues demonstrated a connection between $p27^{Kip1}$ and Sox2, one of the so called “Yamanaka factors” (Takahashi and Yamanaka, 2006). They observed that cells lacking $p27^{Kip1}$ could be reprogrammed into induced pluripotent stem cells (iPSCs), in absence of ectopic Sox2. Mechanistically, they showed that, upon differentiation, $p27^{Kip1}$ associates to the SRR2 enhancer of the Sox2 gene together with a p130-E2F4-SIN3A repressive complex. Interestingly, cells and tissues from $p27^{Kip1}$ null mice, including brain, lung, and retina, present an elevated basal expression of Sox2, suggesting that $p27^{Kip1}$ could actively contribute to the repression of Sox2 (Li et al., 2012).

2 Aim of the study

The tumor suppressor $p27^{Kip1}$ is involved in different cellular processes, such as proliferation, differentiation, apoptosis, regulation of cytoskeleton and cell migration. Several clinical studies have highlighted that $p27^{Kip1}$ downregulation has prognostic and predictive potential, in various types of human tumors, particularly in BC. In the Luminal subtype, mutations at the C-terminal region of $p27^{Kip1}$ have been identified as driver genetic lesions. Furthermore, it has been reported that $p27^{Kip1}$ expression could predict LBC patients' sensitivity to endocrine-, chemo- and anti-HER2 therapies. Thus, dissecting the role of $p27^{Kip1}$ and its domains in LBC onset, progression and response to therapies represent an important objective. This is especially true for the luminal B subtype, which, compared to the luminal A, presents an aggressive clinical behavior still difficult to manage by clinicians.

The first aim of this PhD project was to develop and characterize a luminal B BC cell line genetically modified for $p27^{kip1}$ expression. To this aim, we chose the poorly tumorigenic MCF-7 LBC cell line and, exploiting the Zinc Finger Nucleases technology, we generated $p27^{kip1}$ Knock-Out (KO) clones. Next, we used a $p27^{kip1}$ KO clone to Knock-In (KI) the K134fs and T171* $p27^{kip1}$ mutants, representing two of the driver mutations identified in LBC.

Thereafter, through different techniques and functional assays, we assessed whether loss or mutation of $p27^{kip1}$, in the KO and KI clones, altered the behavior of MCF-7 cells.

The main goal was testing the response of the different $p27^{kip1}$-modified MCF-7 cells to the LBC patients' standard of care therapies, which mainly consist in endocrine- and radiotherapy. The characterization of the role of $p27^{kip1}$ in the response to endocrine treatment is still in progress. In collaboration with the Radiotherapy Unit of our Institute, we thus explored the response of MCF-7 cells to γ-radiation, focusing on MCF-7 $p27^{kip1}$ KO and KI clones ability to repair the DNA damage induced by γ-radiation, to maintain their genome stability and survive.

3 Results

3.1 Generation of a luminal breast cancer cell line modified for $p27^{kip1}$

Given the complexity and importance to study $p27^{kip1}$ in LBC, the first goal of the project was the generation of CDKN1B (the gene encoding for $p27^{kip1}$) Knock-Out (KO) and mutant CDKN1B Knock-In (KI) BC epithelial cells. To this aim, we chose the MCF-7 (ER+/PR+) luminal B BC cell line, which responds to nutrient deprivation, cell-cell contact and TGFβ treatment by up-regulating $p27^{kip1}$ nuclear expression. We genetically manipulated the MCF-7 cells using the Zinc Finger Nucleases (ZFNs) technology, as reported in Figure 1A. This technique involves the use of a pair of engineered zinc finger proteins, capable of recognizing in a highly specific manner two adjacent sequences of DNA, linked to FokI, a non-specific nuclease, able to cleave the dsDNA between the two sequences. The breakage of the DNA evokes endogenous repair mechanisms: the cleaved ends may be joined back together in an error prone process called non homologous end-joining (NHEJ); otherwise the other allele or an exogenous template may be used to repair the break by homology directed repair (HDR).

During NHEJ, the broken ends are joined inaccurately, creating deletions, insertions, and substitutions at the break site, resulting in the expression of a truncated and/or nonfunctional protein. To generate CDKN1B KO MCF-7 cells we first transfected MCF-7 cells, by electroporation, with DNA of the ZFNs engineered to target the CDKN1B gene sequence. Following single cell cloning and screening, we obtained clones heterozygous for $p27^{kip1}$, as confirmed by Cell One assay, fragment cloning and sequence and Western Blot analyses. Since the analysis of MCF-7 chromosomal map, demonstrated that this cell line has a complex karyotype with 4 to 7 chromosome 12, where CDKN1B is located (not shown), we decided to re-transfect one of the obtained $p27^{kip1}$ heterozygous clones then subjected to a second round of single cell cloning and screening. Using this approach, we isolated two MCF-7 $p27^{kip1}$KO clones named #8 and #17.

The disruption of the CDKN1B gene was confirmed by NGS, Sanger sequence (Figure 1B) and western blot analysis (Figure 1D). As experimental controls, we selected two different clones that resulted WT for $p27^{kip1}$ during the entire process of clonal selection.

Then, we took advantage of the HDR pathway to generate the MCF-7 $p27^{kip1}$ KI clones. We delivered by electroporation into the MCF-7 $p27^{kip1}$KO #17 clone, a template donor, consisting in $p27^{kip1}$ WT or mutant constructs, and the mRNA of specific ZFN. We directed

the integration of $p27^{kip1}$ and of two mutants of our interest into the AAVS1 site (adeno-associated virus integration site 1), located in human chromosome 19 and considered a safe harbor locus for gene-targeted integration.

The two mutants, recently identified in LBC (Ellis et al., 2012), were the frameshift (fs) mutation at the 134 aminoacid of $p27^{kip1}$ ($p27^{kip1}$ K134fs), which leads to expression of a truncated form of the protein which lacks the nuclear localization signal (NLS) and a nonsense mutation at the 171 aminoacid of $p27^{kip1}$ ($p27^{kip1}$ T171*) that create a new stop codon just after $p27^{kip1}$ NLS.. The structure of $p27^{kip1}$ protein and the localization of the mutations in $p27^{kip1}$ sequence are reported in Figure 2C.

We screened more than 200 clones for each mutant, first by PCR and then by western blot analysis, and in this manner we selected two clones expressing the $p27^{kip1}$ WT, three clones expressing the mutant $p27^{kip1}$ K134fs and two $p27^{kip1}$ T171*.

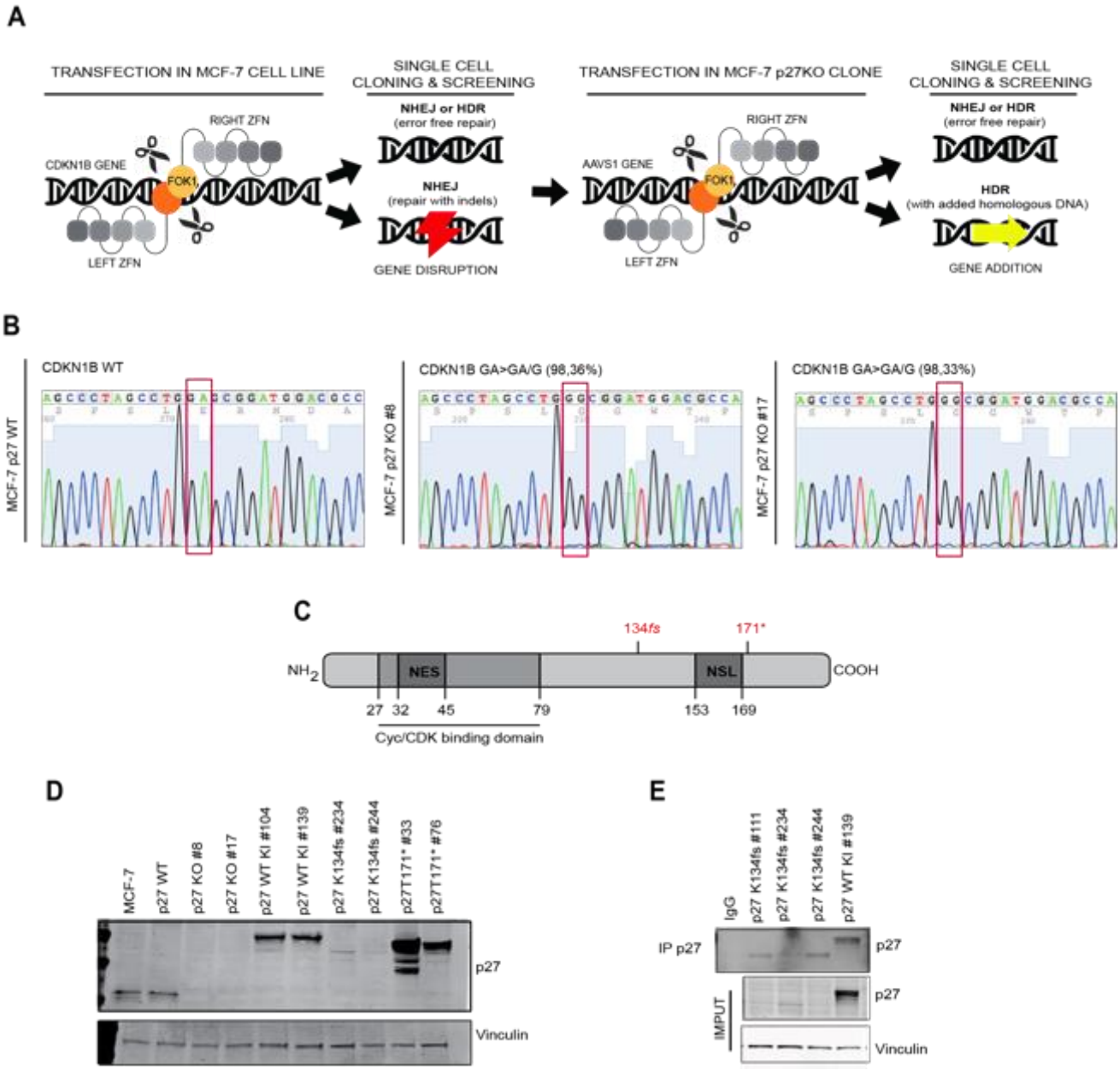

Figure 1. Generation of MCF-7 p27^{kip1} KO and p27^{kip1} mutant KI. **A.** Picture depicts the experimental workflow followed to generate the clones. ZFN, zinc fingers nucleases; DSB, double strand breaks; NHEJ, non-homologous end joining; HDR, homologous directed repair; AAVS1, Adeno-Associated Virus Integration Site 1. **B.** Representative images of the DNA sequence, evaluated by Sanger method, corresponding to CDKN1B gene, showing the WT and the mutated sequences in two p27^{kip1} KO clones (#8 and #17). The two clones both display a single base deletion GA>GA/G in the 98,36% and 98,33% respectively of the analyzed reads (2629 total reads for the p27^{kip1} KO #8; 1495 total reads for p27^{kip1} #17) in the NGS analysis **C.** Schematic representation of p27^{kip1} protein structure. Frameshift (fs) mutation at aminoacid 134 and nonsense (*) mutation at aminoacid 171 are depicted in red. **D.** Western blot analyses of p27^{kip1} expression in protein lysates collected from MCF-7 parental cells, and p27^{kip1} WT-, p27^{kip1}KO- clones **E.** Western blot analyses of p27^{kip1} expression in protein lysates collected from the different p27^{kip1}KI MCF-7 cell clones, expressing p27^{kip1}WT, p27^{kip1}K134fs or p27^{kip1}E171*, as indicated.

3.2 Impact of $p27^{Kip1}$ on MCF-7 cell behavior, in 2D-culture conditions

3.2.1 Characterization of the proliferative behavior of $p27^{kip1}$-modified MCF-7 cells

To analyze the effect of the $p27^{kip1}$ KO and the expression of the $p27^{kip1}$ mutants during cell cycle progression and given that $p27^{kip1}$ is a major regulator of the G1-S phase transition, we serum starved cells for 36 hours to accumulate them in G1 phase and then stimulated cell cycle enter by releasing cells in complete medium (Figure 2A). The re-entry in the cell cycle was analyzed by FACS analysis of the DNA content, by propidium iodide staining. Data showed that $p27^{kip1}$ KO MCF-7 clones were poorly affected by the starvation and re-entered rapidly in the cell cycle, while the re-expression of $p27^{kip1}$ WT reverted this phenotype showing a behavior similar to the parental and the $p27^{kip1}$ WT cell lines. In fact, the percentage of the $p27^{kip1}$ KO MCF-7 cells in the G1 phase of the cell cycle after 36 hours of starvation is 62,9% vs. the 70-75% of the MCF-7, MCF-7 $p27^{kip1}$ WT and MCF-7 $p27^{kip1}$ WT KI. Only after 18 hours of release the clones expressing the WT form of $p27^{kip1}$ showed a comparable cell cycle phase distribution of their exponentially growing state, while the MCF-7 $p27^{kip1}$ KO cells re-entered completely in cycle only after 9 hours of release. The clones expressing the $p27^{kip1}$ T171* mutant, which maintains the nuclear localization signal (NLS) of the protein, were sensible to the starvation and gradually re-entered in the cell cycle after release in complete medium. The $p27^{kip1}$ K134fs expressing clones that do not retain the NLS of $p27^{kip1}$, were mildly influenced by starvation and rapidly re-entered in the cell cycle. These data demonstrated that $p27^{kip1}$ plays an important role in the control of cell cycle progression of MCF-7 cells and that, in these cells, it has a major function in the transition between G1 and S phase.

We next verified whether this altered G1-S transition observed in $p27^{kip1}$KO MCF-7 translated into increased proliferation, using growth curve assays. Although a reproducible increase of the cell number in $p27^{kip1}$ KO clones with respect to the controls was consistently detected, this increase was not statistically significant, indicating that the KO of $p27^{kip1}$ did not substantially affect the proliferation rate of MCF-7 cells under normal culture conditions (Figure 2B). On the other hand, we found that re-expression of $p27^{kip1}$ (MCF-7 $p27^{kip1}$ KI WT) induced a strong inhibition of proliferation, probably due to the high and constitutive expression levels reached in these clones by $p27^{kip1}$, that is transcribed under a CMV promoter.

A

MCF-7

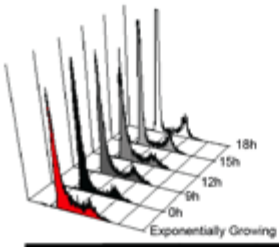

	sub. G1	G1	S	G2-M
Exp. Growing	0,5	55,4	23,5	20,2
0h	0,7	75	8,3	15,7
9h	0,9	65,8	13	19,5
12h	1,6	65,6	12,8	19,2
15h	0,5	68,7	16,1	14,1
18h	0,3	64,6	18	16,8

MCF-7 p27 WT

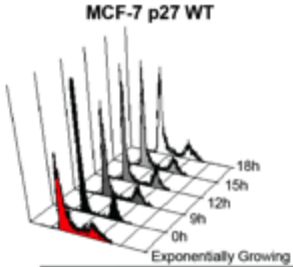

	sub. G1	G1	S	G2-M
Exp. Growing	0,3	58,2	29	12,5
0h	0,4	74	15,8	9,7
9h	0,2	65,1	20,3	14,2
12h	0,5	61,4	25	12,9
15h	0,2	65,4	17,9	16,1
18h	0,2	64,9	16	18,7

MCF-7 p27 KO

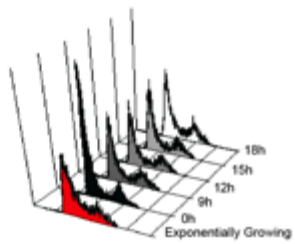

	sub. G1	G1	S	G2-M
Exp. Growing	0,4	52,5	30,8	16,2
0h	0,6	62,9	21,6	14,5
9h	0,6	48,2	32,1	19,2
12h	0,9	42,4	39	17,7
15h	1,1	43,2	38,7	17
18h	0,1	48,2	31,6	20

MCF-7 p27 WT KI

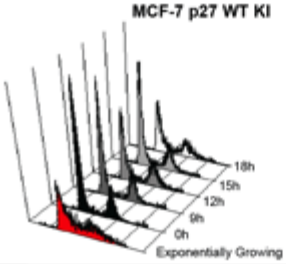

	sub. G1	G1	S	G2-M
Exp. Growing	0,2	36,7	36,3	27,3
0h	0,6	60,6	16,6	21,5
9h	0,4	51,7	20,9	25,3
12h	0,6	44,4	25,2	28,8
15h	0,7	49,5	25,4	24
18h	0,5	41,1	32,8	24,9

MCF-7 p27 K134fs KI #111

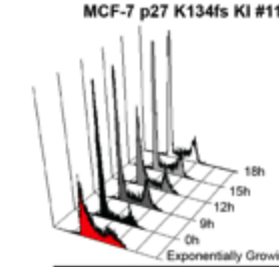

	sub. G1	G1	S	G2-M
Exp. Growing	0,8	33,8	43,6	21,8
0h	0,9	60,1	21,7	16,9
9h	0,6	53,2	21,1	25
12h	0,7	48	30	21,3
15h	0,9	60,1	22,4	16,4
18h	0,6	61,7	16,5	21

MCF-7 p27 K134fs KI #234

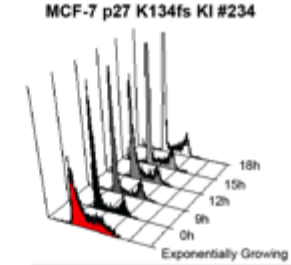

	sub. G1	G1	S	G2-M
Exp. Growing	0,1	38	39,5	22,3
0h	0,4	66,9	15	17
9h	0,3	64,6	19	15,6
12h	0,6	51,6	30	17,8
15h	0,8	66,7	14,4	17,8
18h	0,4	64,4	17,1	17,7

MCF-7 p27 T171* KI #33

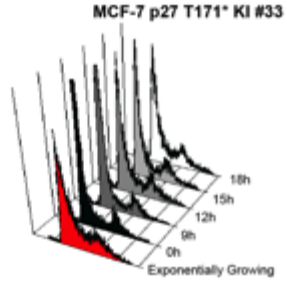

	sub. G1	G1	S	G2-M
Exp. Growing	1,11	52,04	28,36	21,15
0h	2,16	60,22	19,17	18,05
9h	1,59	66,36	17,65	16,37
12h	2,75	57	21,06	20,92
15h	2,87	54,51	24,95	19,7
18h	0,99	53,67	19,05	27,6

MCF-7 p27 T171* KI #76

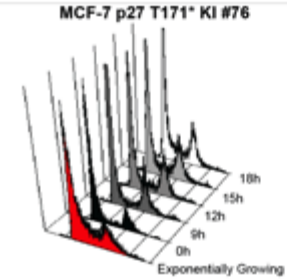

	sub. G1	G1	S	G2-M
Exp. Growing	1,11	52,04	28,36	21,15
0h	2,16	60,22	19,17	18,05
9h	1,59	66,36	17,65	16,37
12h	2,75	57	21,06	20,92
15h	2,87	54,51	24,95	19,7
18h	0,99	53,67	19,05	27,6

B

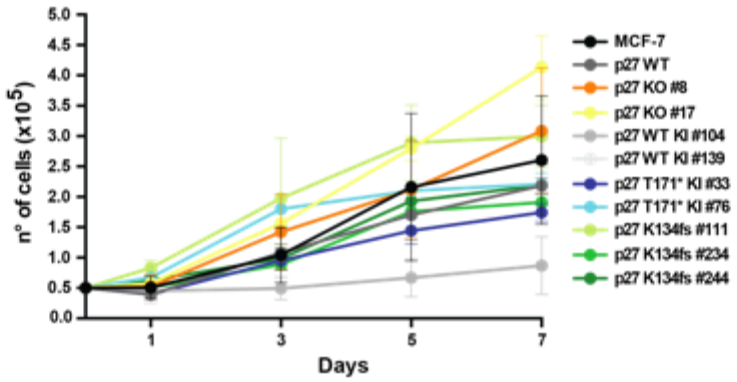

Figure 2. Loss of $p27^{kip1}$ does not significantly affect the proliferative phenotype of MCF-7 in basal culture conditions. A. FACS analysis after PI staining of the DNA of cell cycle distribution after starvation and release in complete medium. Cells were harvested in exponentially growing condition, after starvation and after 9h, 12h, 15h, 18h of serum release. The percentages of the cells in each phase are reported in the tabs under the respective histogram plot. **B.** Growth curve analysis of MCF-7 $p27^{kip1}$KO and $p27^{kip1}$KI clones. 0,5x 10^5 cells/well were plated in duplicate in complete medium at day 0 and then counted by Trypan Blue exclusion test, at the indicated days.

3.2.2 Characterization of 2D motility

Given the already established involvement of $p27^{kip1}$ in the regulation of cell motility (Baldassarre et al., 2005; Daniel et al., 2004; Goukassian, 2001; Sun et al., 2001) we tested the effect of loss of $p27^{kip1}$ or expression of $p27^{kip1}$ K134fs or T171* mutation on MCF-7 cells random motility (Figure 3A, 3B and 3C) and the scratch-covering ability (Figure 3D), using time-lapse microscopy. Loss of $p27^{kip1}$ did not significantly alter the ability of MCF-7 cells to move in 2D, respect the MCF-7 control cells, both in terms of distance covered and velocity of migration (Figure 3B and 3C).

Together, the results from these experiments indicate that $p27^{kip1}$ plays a role in the control of cell cycle progression of MCF-7 cells, but it doesn't substantially affect their proliferation and motility in 2D-culture conditions.

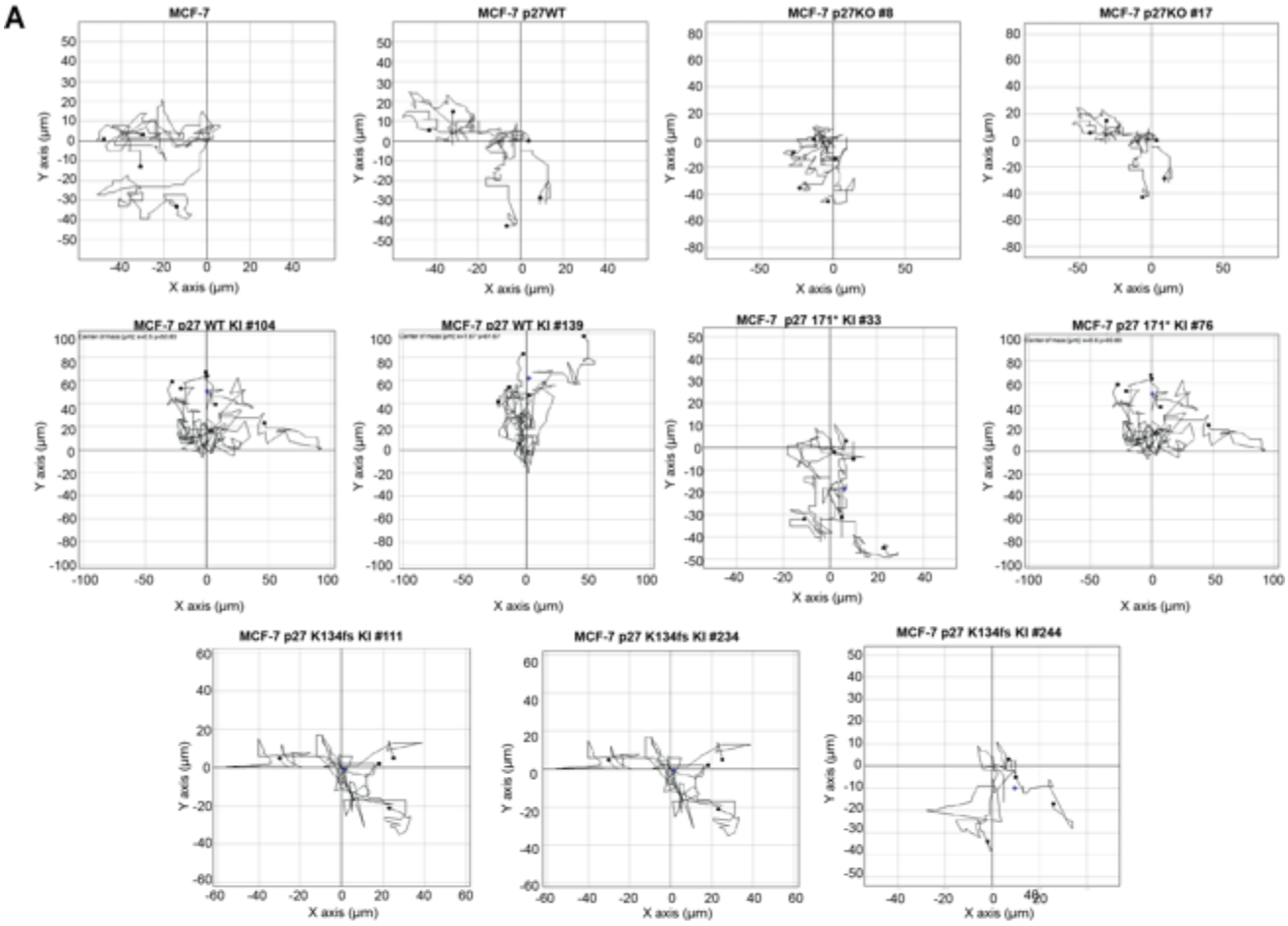
A
MCF-7
MCF-7 p27WT
MCF-7 p27KO #8
MCF-7 p27KO #17
MCF-7 p27 WT KI #104
MCF-7 p27 WT KI #139
MCF-7 p27 171* KI #33
MCF-7 p27 171* KI #76
MCF-7 p27 K134fs KI #111
MCF-7 p27 K134fs KI #234
MCF-7 p27 K134fs KI #244
Y axis (µm)
X axis (µm)

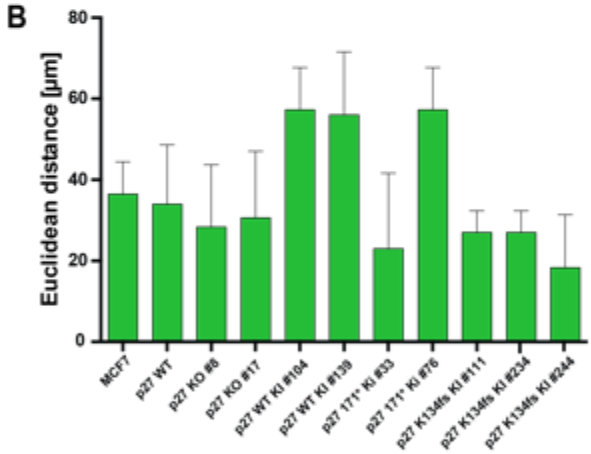
B
Euclidean distance [µm]
MCF7
p27 WT
p27 KO #8
p27 KO #17
p27 WT KI #104
p27 WT KI #139
p27 171* KI #33
p27 171* KI #76
p27 K134fs KI #111
p27 K134fs KI #234
p27 K134fs KI #244

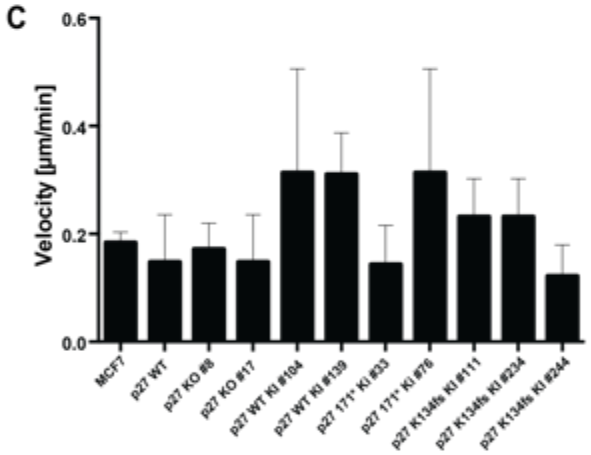
C
Velocity [µm/min]
MCF7
p27 WT
p27 KO #8
p27 KO #17
p27 WT KI #104
p27 WT KI #139
p27 171* KI #33
p27 171* KI #76
p27 K134fs KI #111
p27 K134fs KI #234
p27 K134fs KI #244

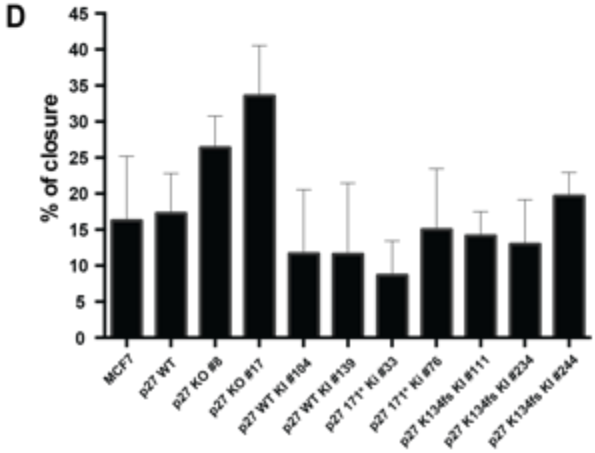
D
% of closure
MCF7
p27 WT
p27 KO #8
p27 KO #17
p27 WT KI #104
p27 WT KI #139
p27 171* KI #33
p27 171* KI #76
p27 K134fs KI #111
p27 K134fs KI #234
p27 K134fs KI #244

Figure 3. Loss of $p27^{kip1}$ does not significantly affect the 2D-motility of MCF-7 cells. After time-lapse video microscopy of MCF-7 clones plated 6x 10^3 cells/well to tracking their random motility, the analysis of the distance covered (**B**) and velocity (**C**) was performed using a semi-automatic cell tracking software. Two independent experiments were performed and 6 cells for each cell lines were tracked in each experiment. The rose plot reported in **A** is representative of the distance covered by the clones. In **D** the graph reports the % of the scratch closure. Cells were plated as monolayer and scratched with a yellow tip. The distance between the edges was measured at the beginning and at the end of the assay, then compared to verify the % of scratch covering. In both assays cells were followed for 15 hours collecting one picture every 5 minutes.

3.3 Impact of $p27^{kip1}$ on MCF-7 cell behavior, in 3D-culture conditions

3.3.1 Evaluation of proliferation in anchorage independence

We next investigated if and how the expression of $p27^{kip1}$ WT, $p27^{kip1}$K134fs or $p27^{kip1}$ T171* could impinge on the tumorigenic potential of MCF-7 cell. A typical hallmark of transformed cells is the ability to grow in anchorage independence. We evaluated the capacity of our clones to grow in soft agar in complete medium or in reduced serum medium (2,5%) (Figure 4). In both conditions, loss of $p27^{kip1}$ induced a significant increase in both number (Figure 4A) and size of colonies (Figure 4C and 4D) grown in soft agar, thus suggesting a strong increase in the tumorigenic potential of MCF-7 cells. The reintroduction of the WT form of $p27^{kip1}$ reverted this phenotype, while the mutant-expressing clones displayed a KO-like behavior in terms of size and number of colonies grown in either experimental conditions.

Ongoing experiments will establish whether this increased transformed potential observed *in vitro* effectively results in increased tumor take rate *in vivo,* in mice.

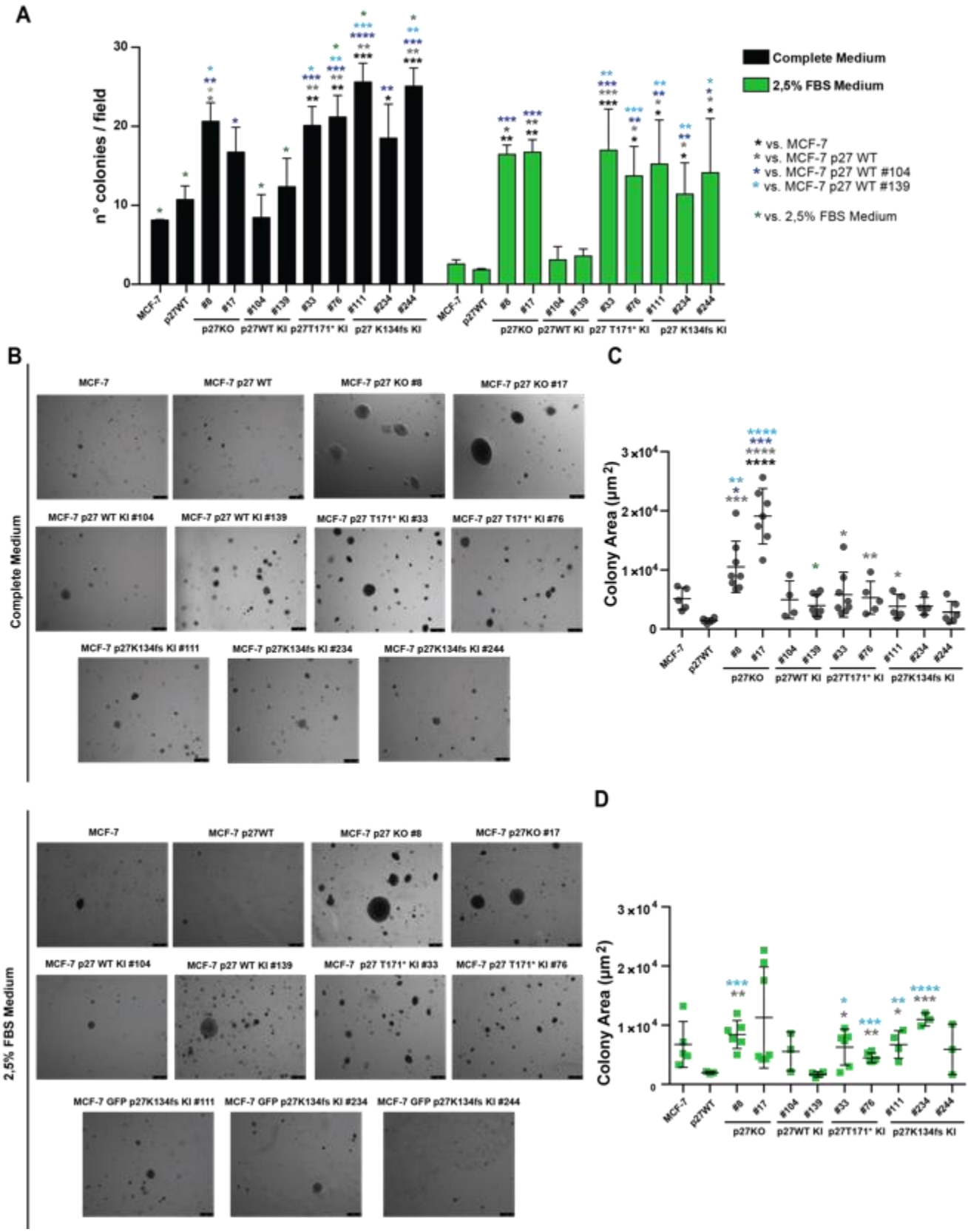

Figure 4. Loss of p27^{kip1} increases the transformed phenotype of MCF-7 cells. A. Graph reports the growth in soft agar assay of different MCF-7 cell clones in complete medium or in a medium with 2,5% of serum. Data was obtained counting, with 10x objective, the colonies in 9 fields for each cell lines (***=p<0,05; ****=p<0,01; *****=p<0,005; ******=p<0,001)*. **B.** Representative photos of colony size using a 30X objective. Graphs reports the area of the colonies grown in complete medium **(C)** and in 2,5% FBS medium **(D)**.

3.3.2 Characterization of growth in mammosphere

Evidences from literature indicate that $p27^{Kip1}$ plays an active role in the maintenance of the stemness-state and during cell differentiation (Baldassarre et al., 1999; Burton et al., 1999; Cheng, 2000; Gao et al., 1997; Li et al., 2012; Matsu-ura et al., 2016; Nguyen, 2006; Nguyen et al., 2006). Cancer stem cells represent a small population within the bulk of the tumor cells, requiring reliable and reproducible control of the self-renewal/differentiation axis to grow.

In order to understand if $p27^{kip1}$ or its loss could confers or supports the stem-like properties to MCF-7 cells, we looked to the ability of the different cell clones to grow and survive as mammospheres, when plated in appropriate medium in polyHEMA-coated plates. In contrast to the standard adherent 2D-culture of cancer cells, this type of 3D-culture selectively exploits inherent biologic features of cancer stem cells, such as anoikis resistance and self-renewal. Stem cell activity is calculated from primary mammosphere formation as percentage of mammosphere forming efficiency (MFE), the ratio between the number of mammospheres per well and the cells seeded. Then, the self-renewal ability is obtained as the ratio between the total number of secondary (or tertiary, etc) mammospheres and the total number of primary mammospheres generated (Shaw et al., 2012). We tested the MFE of the different clones, plating them either in standard mammospheres media or in post-surgery wound fluids (WF), which are drainage fluids collected from BC patients after primary tumor removal. WF are rich in cytokines and growth factors that strongly stimulate the stem-like phenotype of BC cells (Segatto et al., 2014). Our data clearly indicated that lack of $p27^{kip1}$ increased the mammosphere forming efficiency, in both first and second generations passages (Figure 5A). Also the self-renewal ability (Figure 5A) of MCF-7 cells and the size of the spheres (Figure 5B, 5C and 5D), especially in presence of WF, were increased by loss of $p27^{kip1}$. This effect was specifically induced by loss of $p27^{kip1}$, since it was abrogated in the $p27^{kip1}$ WT KI clone. It is interesting to note that while the $p27^{kip1}$ 171* KI showed a phenotype comparable with the parental cell line, the $p27^{kip1}$ K134fs mutant displayed an intermediate behavior both in terms of MFE and size of mammospheres, suggesting that this could be a nuclear function of $p27^{kip1}$.

Together, the results from the experiments carried out in 3D-culture conditions indicate that the KO of $p27^{kip1}$ impacts on the transformed phenotype and stem-like properties of MCF-7 cells, conferring a more oncogenic potential.

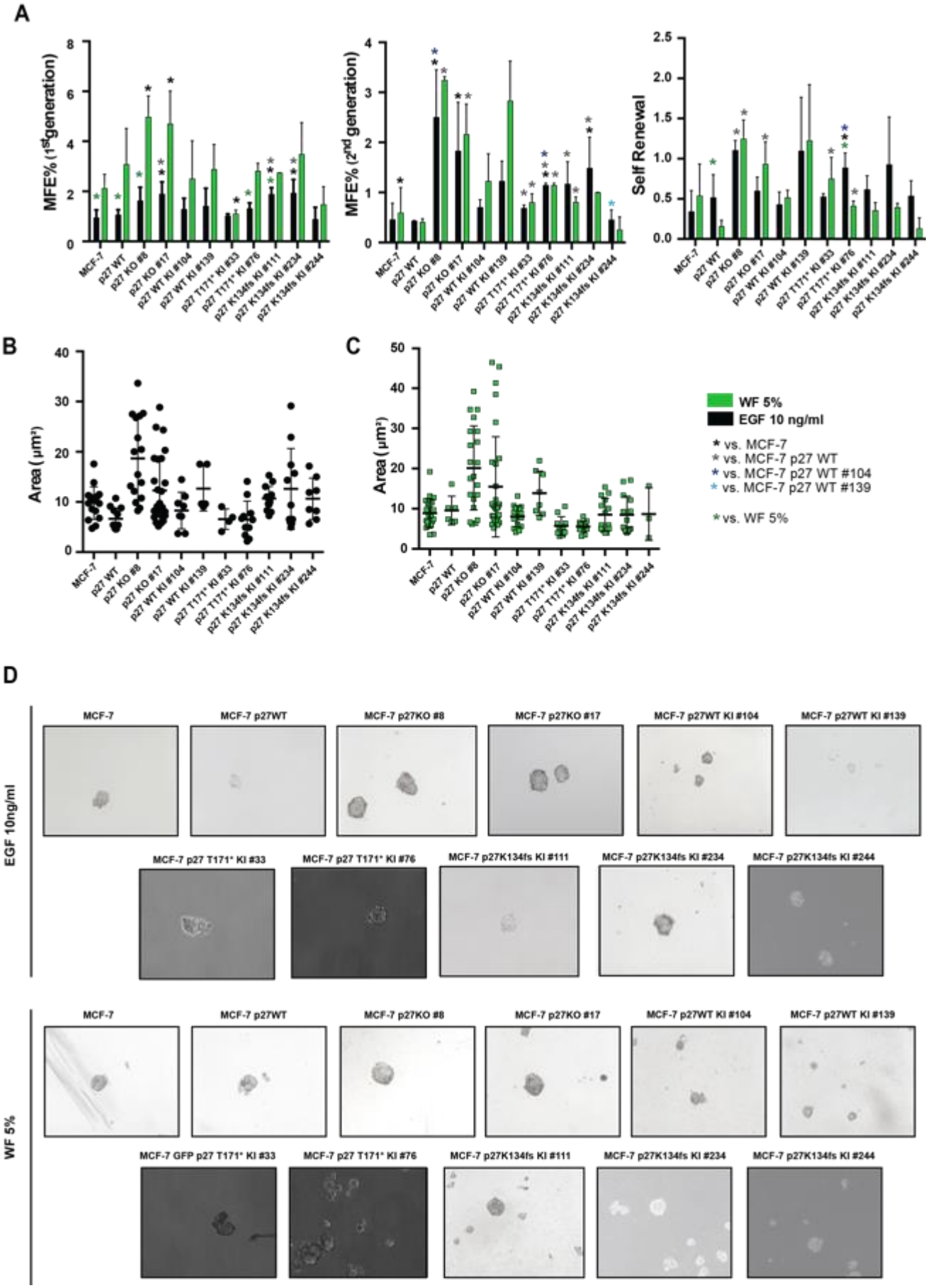
A
MFE% (1st generation)
MFE% (2nd generation)
Self Renewal
MCF-7
p27 WT
p27 KO #8
p27 KO #17
p27 WT KI #104
p27 WT KI #139
p27 T171* KI #33
p27 T171* KI #76
p27 K134fs KI #111
p27 K134fs KI #234
p27 K134fs KI #244
B
Area (µm²)
C
Area (µm²)
WF 5%
EGF 10 ng/ml
* vs. MCF-7
* vs. MCF-7 p27 WT
* vs. MCF-7 p27 WT #104
* vs. MCF-7 p27 WT #139
* vs. WF 5%
D
EGF 10ng/ml
WF 5%
MCF-7
MCF-7 p27WT
MCF-7 p27KO #8
MCF-7 p27KO #17
MCF-7 p27WT KI #104
MCF-7 p27WT KI #139
MCF-7 p27 T171* KI #33
MCF-7 p27 T171* KI #76
MCF-7 p27K134fs KI #111
MCF-7 p27K134fs KI #234
MCF-7 p27K134fs KI #244
MCF-7 GFP p27 T171* KI #33

Figure 5. Loss of p27^{kip1} increases the stem-like properties of MCF-7 cells. A. Graph reports the MFE of first and second generation and self renewal ability of MCF-7 clones, in mammosphere assays performed in presence of EGF 10ng/ml or 5% wound fluids (WF), as indicated. The areas of the 2nd generation colonies formed by the clones cultured as mammospheres in presence of EGF 10ng/ml or 5% wound fluids are reported in the graphs **B** and **C**, respectively. **D.** Typical images of mammospheres from MCF-7 and MCF-7-modified clones are reported.

3.4 Impact of $p27^{kip1}$ on MCF-7 cell response to γ-radiation

Cassimere and colleagues have recently demonstrated that $p27^{kip1}$ is involved in the delay of G1/S transition after γ-radiation (Cassimere et al., 2016). Other studies point to a role of $p27^{kip1}$ in the G2/M checkpoint arrest, in response to prolonged exposure to DNA breaks, preventing the damaged DNA to be inherited by daughter cells (Cuadrado et al., 2009; Deckbar et al., 2011; Nakayama et al., 2004; Payne et al., 2008). Recent studies in esophageal cancers showed that downregulation $p27^{Kip1}$ could have a potential predictive role in γ-radiation responsiveness, conferring radioresistance to the cancer cells (Tong et al., 2011; Wang et al., 2012).

Given that γ-radiation is an integral part of the standard therapy proposed to luminal B BC patients and given $p27^{Kip1}$ putative role in maintaining genome integrity, we tested the response of MCF-7 clones to γ-radiation.

First, we analyzed if expression of $p27^{Kip1}$ was associated with a different extent of survival γ-radiation performing a series of clonogenic assays.

To evaluate whether loss of $p27^{Kip1}$ or expression of the mutants could confer a growth advantage *per se*, independently from the resistance/sensitivity to γ-radiation, we established the plating efficiency (PE) of each cell clone. To this aim, we plated four different cell concentrations, let them grow in complete medium for 15 days, then stained the colonies with crystal violet and counted them.

	100			200			400			800			
MCF-7	0	2	2	3	3	3	3	8	6	9	11	15	n° cells plated
													n° colonies counted
	1,333333			3			5,666667			11,66667			n° colonies/well
	1%			2%			1%			1%			n° colonies/cells plated
MCF-7 p27^{Kip1} WT	1	1	1	5	3	3	3	6	8	6	6	6	n° colonies counted
	1			3,666667			5,666667			6			n° colonies /well
	1%			2%			1%			1%			n° colonies /cells plated
MCF-7 p27^{Kip1} KO #8	13	16	9	30	20	30	39	47	36	65	60	63	n° colonies counted
	12,66667			26,66667			40,66667			62,66667			n° colonies /well
	13%			13%			10%			8%			n° colonies /cells plated
MCF-7 p27^{Kip1} KO #17	12	7	10	15	23	12	44	34	38	61	52	50	n° colonies counted
	9,666667			16,66667			38,66667			54,33333			n° colonies /well
	10%			8%			10%			7%			n° colonies /cells plated
MCF-7 p27^{Kip1} WT KI	0	2	2	3	1	2	4	6	6	6	8	5	n° colonies counted
	1,333333			2			5,333333			6,333333			n° colonies /well
	1%			1%			1%			1%			n° colonies /cells plated
MCF-7 p27^{Kip1} K134fs KI	2	5	4	6	3	5	8	6	7	4	6	7	n° colonies counted
	3,666667			4,666667			7			5,666667			n° colonies /well
	4%			2%			2%			1%			n° colonies /cells plated

	average	St. Dev.
MCF-7	1,43%	0,07%
MCF-7 p27^{Kip1} WT	1,25%	0,48%
MCF-7 p27^{Kip1} KO #8	11,00%	2,51%
MCF-7 p27^{Kip1} KO #17	8,61%	1,37%
MCF-7 p27^{Kip1} WT KI	1,11%	0,27%
MCF-7 p27^{Kip1} K134fs KI	2,11%	1,23%

Tab 1. MCF-7 clones plating efficiency.

As reported in Table 1, the PE for all clones was approximately 2%, with the exception of the MCF-7 p27^{kip1} KO clones, which showed a PE of 8%-10%. This result already indicated that under challenging culture condition, such as in clonogenic assay, loss of p27^{kip1} provides a survival advantage to MCF-7 cells. We exploited this information to design our clonogenic assays, as described in particular in Materials and methods section. Thanks to the collaboration with the Radiotherapy Unit of our Institute, we had the possibility to use the linear accelerator for External Beam Radiation Therapy (CLINAC 600c, Varian). We irradiated the MCF-7 clones with the two different doses of γ-radiation, 2Gy and 5Gy (Figure 6A).

We found more important differences between the MCF-7 with modified expression of $p27^{kip1}$ after the low dose of γ-radiation (Figure 6B). This data confirm what has been already reported in literature by Payne and colleagues, that is after high doses the mechanisms responsible for DNA repair and survival do not likely involved $p27^{kip1}$ (Payne et al., 2008). MCF-7 $p27^{kip1}$ KO cells showed a higher survival fraction (evaluated as number of colonies formed after γ-radiation divided the number of cells seeded and the clone PE) than the control cells; also the MCF-7 $p27^{kip1}$K134fs clones demonstrated to have an advantage in survival than the cells expressing the WT form of $p27^{kip1}$, but not with the same entity of $p27^{kip1}$KO cells.

Given this result and the fact that the dose of 2Gy represents a clinically more relevant dose in BC therapy, frequently used in the hyper-fractionated radiotherapy regimens, we decided to focus our characterization in this γ-radiation dose. As a measure for chromosomal damage, we analyzed the expression of the phosphorylated form of histone H2AX (Ser139-H2AX, *i.e.* γH2AX), a very sensitive and well-established marker for DNA double-strand breaks (DSBs). We analyzed the number of cells positive for γH2AX foci by immunofluorescence, after 1 hour and 24 hours from γ-radiation. At the early time point (1h), all clones presented a similar number of cells positive for γH2AX foci (Figure 6C and 6D). However, when we looked at the residual DNA damage 24 hours after γ-radiation, we found a significant reduction in γH2AX foci (in terms of number of γH2AX positive cells) in MCF-7 cells expressing $p27^{kip1}$WT compared to $p27^{kip1}$ null cells (Figure 6C and 6D), suggesting a prolonged retention of un-repaired DSB in the absence of $p27^{kip1}$. Interestingly, we found that cells expressing the mutant form of $p27^{kip1}$ K134fs displayed a behavior similar to MCF-7 $p27^{kip1}$ KO cells, counting significantly higher γH2AX residual foci compared to $p27^{kip1}$ WT and $p27^{kip1}$ WT KI clones (Figure 6C and 6D).

Unrepaired DSBs can be responsible for mitotic defects and are ultimate lesions for the formation of chromosomal aberrations. To better study possible mitotic defects associated with loss of $p27^{kip1}$ or with the expression of the mutants, we scored and catalogued hundreds of mitotic cells 48 hours after 2Gy γ-radiation, by staining cells for pSer10-Histone H3 (as marker of mitotic cells) and α-tubulin (as marker of the mitotic spindle).

As expected, non-γ-radiated proliferating cells displayed a very low number of aberrant mitoses, with no remarkable differences among the clones. After 48 hours from 2Gy γ-radiation, the MCF-7 $p27^{kip1}$ WT expressing clones showed a number of mitotic defects comparable with the untreated counterparts, indicating that DNA damage has been solved and/or cells carrying unrepaired DNA damage have been cleared out. On the contrary,

p27^{kip1} KO cells displayed a significant increment of abnormal mitoses and chromosomal aberrations and the clones expressing the p27^{kip1}K134fs mutant presented a milder phenotype, with a lower number of mitotic defects in comparison to the MCF-7 p27^{kip1} KO cells (Figure 7A and 7B). No remarkable difference in the type of aberrant mitoses and chromosomal defects among the irradiated cells were found.

These data underlined that the presence of p27^{kip1} is important for maintaining the genetic stability of the cells after γ-radiations, also in the MCF-7 LBC cell line model.

Considering the increased genomic instability of p27^{kip1} KO cells and their higher survival rate after DNA damage, we asked whether the mechanisms involved in the cell cycle control, in particular the G2/M checkpoint, in these cells were affected. Following DNA damage, the cyclin B1/CDK1 complex is immediately inactivated, thus avoiding that cells enter in mitosis before the repair of the damaged DNA is completed. To evaluate this process, we performed kinase assay of cyclin B1/CDK1 complexes in the different clones and clearly observed that p27^{kip1} KO cells did not display the necessary drop in kinase activity that was observed in all other p27^{kip1} expressing MCF-7 cells (Figure 7C). In parallel, we evaluated the mitotic index of MCF-7 cells 1 hour after 2Gy γ-radiation using the phosphoSer10-Histone H3 marker. Consistent with above results, MCF-7 p27^{kip1} KO clones displayed higher number of pH3 positive cells respect the control cells (Figure 7D).

Taken together, these data indicate that cells with defective p27^{kip1} expression do not properly activate the G2/M checkpoint after γ-radiation and they are not efficiently cleared out before progressing into the subsequent M phase. In detail, MCF-7 p27^{kip1} KO cells show a higher percentage of unsolved residual DSBs after 24 hours of γ-radiation. These DSBs can be responsible for the higher rate of mitotic defects observable 48 hours after γ-radiation. Moreover, MCF-7 p27^{kip1} KO cells show a survival advantage after γ-radiation respect the MCF-7 p27^{kip1} WT expressing cells, which indicate that p27^{kip1} could also be involved in the mechanisms responsible for the clearing out of the aberrant cells.

In conclusion, absence of p27^{kip1} in MCF-7 luminal cells treated with γ-radiation induces genomic instability and increased cell survival, which could be eventually linked to resistance to radiotherapy.

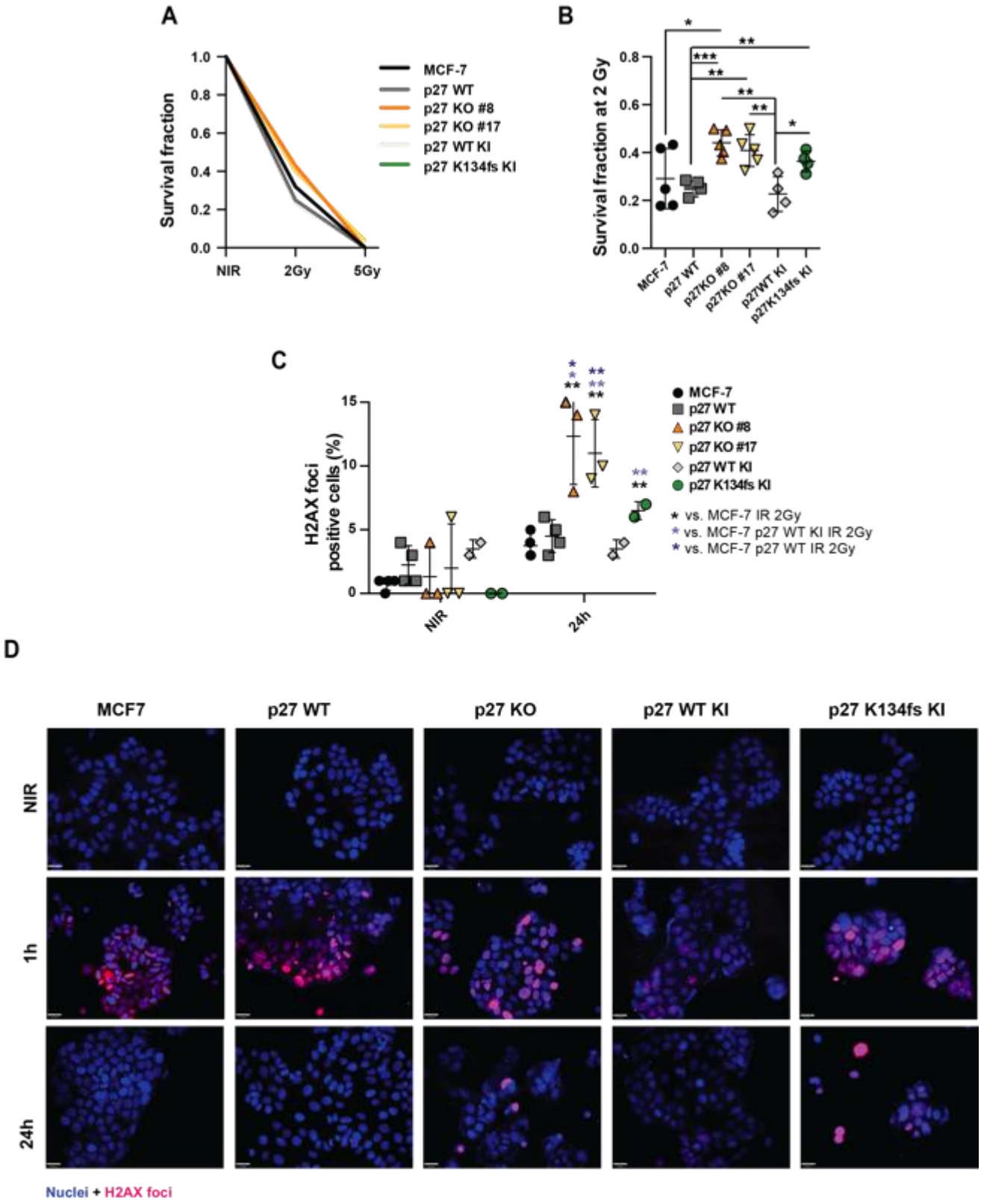

Figure 6. Following γ-radiation, loss of p27^{kip1} increases the radioresistanceresistance and the number of unsolved DSBs. A. and **B.** Graphs report the survival fraction of the different MCF-7 cell clones subjected to 2Gy and 5Gy and then plated in clonogenic assay. * Indicates a p<0.05; ** p<0.01; *** p<0.001. **C.** Graphs report the quantification of the γH2AX positive cells in NIR cell clones and 24 hours after 2Gy, as indicated. **D.** Representative images of cells labeled with propidium iodide (pseudocolored in blue) for the nuclei and with γH2AX (pseudocolored in red) to identify DNA damage positive the cells. 40X objective were used.

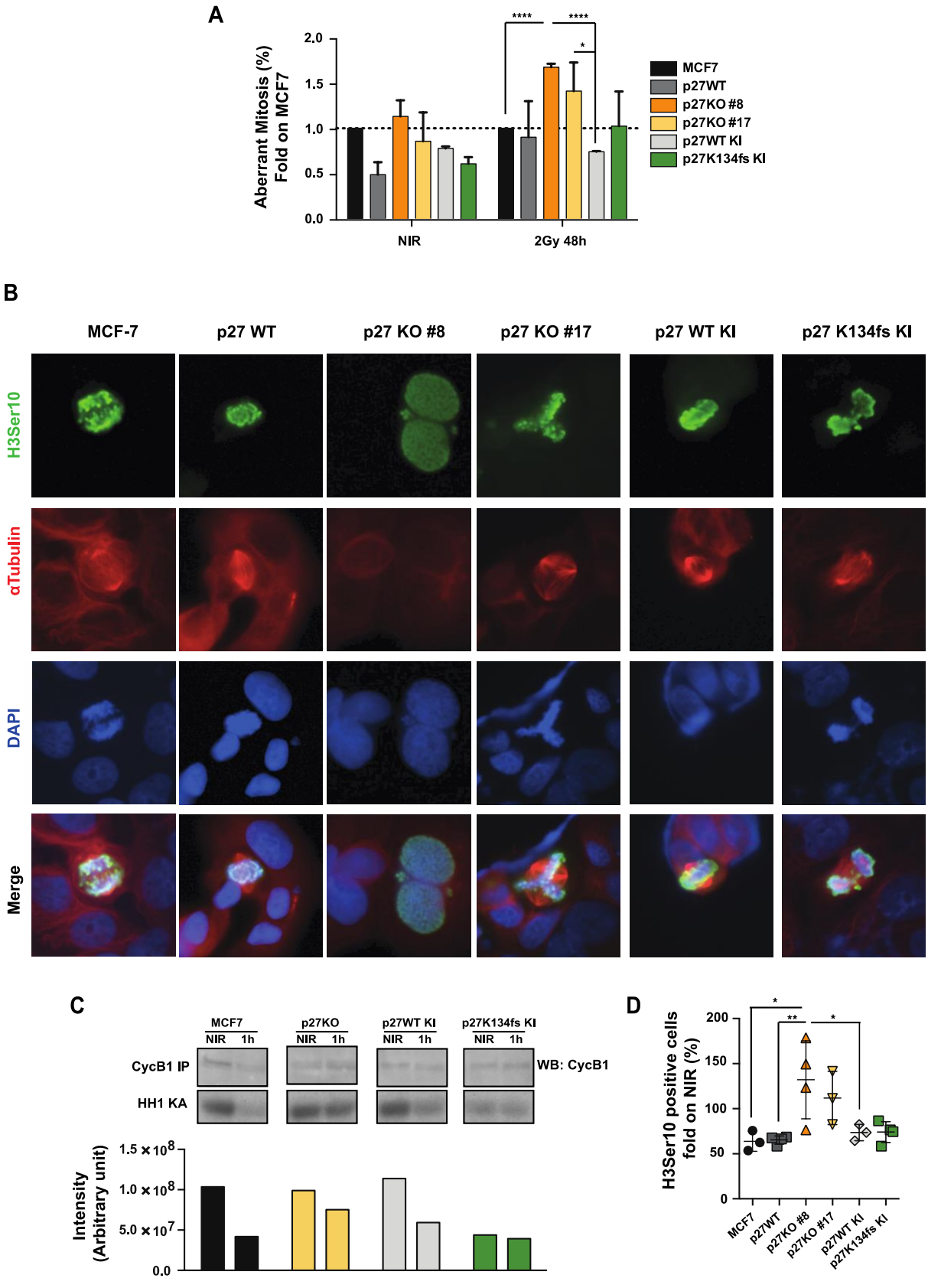
A
Aberrant Mitosis (%)
Fold on MCF7
2.0
1.5
1.0
0.5
0.0
****
****
*
NIR
2Gy 48h
MCF7
p27WT
p27KO #8
p27KO #17
p27WT KI
p27K134fs KI
B
MCF-7
p27 WT
p27 KO #8
p27 KO #17
p27 WT KI
p27 K134fs KI
H3Ser10
αTubulin
DAPI
Merge
C
MCF7
p27KO
p27WT KI
p27K134fs KI
NIR 1h
CycB1 IP
HH1 KA
WB: CycB1
Intensity
(Arbitrary unit)
1.5 x 10^8
1.0 x 10^8
5.0 x 10^7
0.0
D
H3Ser10 positive cells
fold on NIR (%)
200
150
100
50
0
*
**
*
MCF7
p27WT
p27KO #8
p27KO #17
p27WT KI
p27K134fs KI

Figure 7. Following γ-radiation, loss of $p27^{kip1}$ increases mitotic defects and alters G2/M checkpoint. A. Graph reports the quantification of aberrant mitoses displayed by MCF-7 clones, in NIR or 24 hours after 2Gy of IR. Data are expressed as fold increase over the aberrant mitoses found in MCF-7 parental cells. **B.** Representative pictures of cells reporting the above mentioned mitotic aberrations. Cells were stained for phospho-Ser10 Histon-H3 (pS10-H3) to identify mitotic cells (pseudocolored in green). □Tubulin is used to highlight the mitotic spindle and DAPI to identify the cell nuclei. *indicates a $p<0.05$; ** $p<0.01$. **C.** Graph report the kinase assay (KA) on Histon H1 (HH1) by cyclin B1-associated CDK activity (lower panels). Upper panels show the level of immunoprecipitated cyclin B1 in the indicated cell clones. Bottom graph reports the quantification of HH1 phosphorylation, normalized for the quantity of cyclin B1 immunoprecipitated. **D.** Graph reports the quantification of pS3-H3 positive cells, 2 hours after 2Gy, evaluated by counting IF labeled cells, in indicated MCF-7 clones. Data are expressed as fold increase over the value of NIR cells.

4 Materials and Methods

4.1 Generation of luminal BC cell line modified for $p27^{kip1}$

4.1.1 Cell Line

MCF-7 cells were obtained from ATCC (LGC Standards) and grown in DMEM supplemented with 10% FBS. All cell lines were grown in standard conditions at 37ºC and 5% CO_2.

4.1.2 Generation of MCF-7 $p27^{Kip1}$ KO cell clones

Stable $p27^{kip1}$ KO cell clones of MCF-7 cells were obtained by Nucleofection of custom Zinc Finger Nucleases (ZFNs) pair for $p27^{kip1}$ genomic sequence using the AMAXA V kit for electroporation (Lonza), following the manufacturer instruction.

Custom ZFNs targeting the genomic CDKN1B region GGGAGCCCTAGCCTGgagcggATGGACGCCAGGCAG (lower-case letters indicate the cut site) were purchased from Sigma-Aldrich. Following electroporation, cells were maintained at 30°C for 2–3 days, then shifted at 37°C before being single-cell seeded into 96-well plates. The resulting clonal cells were grown in complete media.

4.1.2.1 Surveyor Mutation Detector assay and clonal screening

In order to confirm the ZFN activity in the clones, their genomic DNA was isolated with Lysis solution for Blood and Neutralization solution for Blood (SIGMA) to perform CEL-I assay (Transgenomics Surveyor Nuclease Kit), an enzyme mismatch cleavage assay used to detect single base mismatches or small insertions or deletions. PCR with hp $p27^{kip1}$ ZFN binding primers was used to amplify WT and mutant DNA in the region of ZFN binding (hp $p27^{kip1}$ ZFN binding Fw, 5'-CGTCATTGTCTGAGTAGGTGTCA-3' ; hp $p27^{kip1}$ ZFN binding Rv, 5'-GATCAACCCACCGAGCTGTT-3') The DNA was denatured and re-annealed such that the annealing of WT DNA strand to a mutant strand creates a mismatch "bubble" recognized and cleaved by CEL-I. The cleavage products were detected by 40% acrylamide gel electrophoresis. PCR products from CEL-I positive clones were then cloned into pCR™2.1-TOPO® vector (Invitrogen) and sequenced with M13 primers to confirm deletion (M13 primers: M13Fw, 5'-GTAAAACGACGGCCAG-3'; M13Rv, 5'-CAGGAAACAGCTATGAC-3'). Positive clones, resulted $p27^{kip1}$KO in at least 25 different Sanger sequences, were next analyzed with Western Blot to confirm the absence of $p27^{kip1}$ and, finally, confirmed by Next Generation Sequencing (MySeq V2 Kit, Illumina). Two subsequent rounds of electroporation and single cell cloning were necessary in order

to obtain two different p27KO clones in MCF-7 cells, given that the karyotype of MCF-7 parental cell line used presented 6 copies of chromosome 12 (where CDKN1B reside).

4.1.3 Generation of MCF-7 p27^{Kip1} KI cell clones

To obtain the MCF-7 p27 KI clones, the coding DNA sequence of GFP-p27 WT was cloned downstream a CMV promoter into a pZDonor-AAVS1 vector, a donor plasmid for transgene integration into the human AAVS1 locus (adeno-associated virus integration site 1), located in the human chromosome 19 (SIGMA). The donor vector (pZDonor-AAVS1-GFP-p27WT) was co-transfected by electroporation into one of the two generated p27KO MCF-7 clones, along with the mRNA coding for the ZFN specific for AAVS1 locus (SIGMA). Also in this case, cells were maintained at 30°C for 2–3 days, and at 37°C before being single-cell seeded into 96-well plates. The single-cells cloning were screened by PCR with hp27^{kip1} KI primers (hp27^{kip1} KI Fw, 5'-CATATGTCAAACGTGCGAGTG-3'; hp27^{kip1} KI Rv, 5'-AAGCTTTTACGTTTGACGTCTTCT-3') to verify the integration of p27^{kip1} coding sequence and by Western Blot analysis to verify the protein expression.

4.2 Growth curve and FACS analysis of the cell cycle.

For growth curves, 5x10^4 cells/well were seeded in 6-well plates in complete medium in duplicate. Fresh medium was added every other day. At the indicated times, cells were detached in trypsin-EDTA and counted by Trypan Blue exclusion test.

Cell cycle distribution was analyzed by FACS analysis. Cells were collected and fixed in ice-cold 70% ethanol and maintained at -20°C until ready for the staining procedure. Cells were then washed and resuspended in propidium iodide staining solution (50µg/ml propidium iodide and 0,1mg/ml RNaseA, in PBS 1X). Stained cells were subjected to flow cytometry analysis (FACS) with a FACScan and a FACSCalibur instrument (BD Biosciences). The data were analyzed using WinMDI2.8 software.

4.3 Time-lapse microscopy, quantification of cell motility and scratch covering ability.

MCF-7 clones were plated 6x 10^3 cells/well to tracking their random motility and as monolayer to analyze their ability to recover a scratch. Individual cells or scratch closure on cells' monolayer were monitored by digital bright-field microscopy in order to discriminate cells along the different axes. The pictures were collected every 5 min for 15 hours, using a CCD camera mounted onto the microscope. A 20X objective was used. The cells were maintained at 37°C during all the recording time using a remote temperature

control system and a heating device. At the end of the recording, pictures were used to create a movie (10 images per second, QuickTime), and used for cell tracking analysis or wound healing analysis. After conversion of pixel values into micrometers, single cell motility was quantified by computer-assisted cell tracking of at least 6 selected cells in movement for each experiment, obtaining several locomotion parameters, such as velocity and speed. Velocity describes the actual translocation efficiency of cells in the process of migration, delineating the “true” speed without interference of stopping frequencies. Speed represents a more general parameter describing overall motility as a function of the fraction of locomotion cells and their locomotors duration, individual step lengths and step number. Using the *xyz* coordinates of cell paths, the speed and velocity were calculated by ImageJ Chemotaxis software.

4.4 Anchorage-independent cell growth

To evaluate the cell ability to grow in an anchorage independent manner, soft agar assay was performed. 5×10^3 cells were suspended in 2ml TOP agar medium (DMEM-10%FBS containing 0.4% Low Melting Agarose-SIGMA or DMEM-2,5%FBS containing 0.4% Low Melting Agarose). The cell suspension was then layered on 2ml of jellified BOTTOM agar medium (DMEM-10%FBS containing 0.6% Low Melting Agarose or DMEM-2,5%FBS containing 0.6% Low Melting Agarose) in six-well tissue culture plates in duplicate. DMEM-10%FBS or DMEM-2,5%FBS was added to the plates every 3 days, as a feeder layer. On day 20 the number of colonies was counted in 9 randomly selected fields each well, at 10X magnification.

4.5 Mammospheres assay

To establish primary mammospheres, cells were plated in poly-HEMA coated dishes as single cell suspension (8000 cells in 35 mm dishes). Standard mammosphere medium contains phenol red-free DMEM/F12 (Gibco), B27 supplement (no vitamin A; Invitrogen) and recombinant epidermal growth factor (rEGF, 20 ng/ml; Sigma). Where indicated, cell were plated in medium containing phenol red-free DMEM/F12, B27 supplement and 5% WF. After five days, primary mammospheres were counted using a 4X objective. To establish secondary mammospheres, primary mammospheres were collected, resuspended in 0.5 % trypsin/0.2 % EDTA and disaggregate using 25-gauge needle fitted to a syringe. Cells were plated in the medium at the same seeding density that was used in the primary generation. Mammosphere forming efficiency (MFE%) was calculated as follows: number of mammospheres per well/number of cells seeded per well x 100.

Mammosphere self-renewal was calculated as follows: total number of 2nd mammospheres formed/total number of 1st mammospheres formed.

4.6 Γ-radiation and Clonogenic assay

Γ-radiations were performed using a linear accelerator for External Beam Radiation Therapy cLINAC (cLINAC 600c, Varian) at a dose rate of ~1 Gy/minute at ambient oxygen concentrations and in cell adhesion conditions. Cell plates were first aligned on the positioning table, at the point where the dose administered was maximum, between 2 layers of equal thickness of 'solid water' and irradiated at a dose rate of 2Gy and 5Gy. In every experiment, the dose delivered to the cells by cLINAC was confirmed by radiographic film dosimeter.

Clonogenic assays are commonly used to investigate survival of irradiated cancer cells, and before to perform this investigation we evaluated the plating efficiency (PE) of our clones in standard culture condition. We plated four different concentration of cells (100,200,400,800 cells) in duplicate in 6-well, let them grow in complete medium for 15 days, stained with crystal violet solution (0.5mg/ml crystal violet in 20% methanol). Colonies with more than 50 cells were counted manually and PE was calculated as number of colonies/well divided for the number of cells plated.

For the clonogenic assays to irradiate the number of cells to seed was then calculated using the following formula:

N ° cell = N ° optimal counting colonies / plating efficiency in standard conditions / likelihood of predicted survival

For a 60 mm dish an optimal number of colonies to count is estimated to be 100. The predicted survivals at 2Gy and 5Gy are respectively 50% and 5%.

Cells were seeded in 60 mm dishes (two dilutions, in duplicate) and let adhere to the plates. Cells were then irradiated and maintained at 37ºC and 5% CO_2 for 15 days, refreshing the medium every 3-4 days. Colonies were then fixed and stained with 0.5mg/ml crystal violet in 20% methanol. Colonies with more than 50 cells were counted manually and clonogenic survival fraction (SF) was expressed as the relative plating efficiencies of the irradiated to the control cells.

4.7 Immunofluorescence analysis

MCF-7 cells were grown to sub-confluence on coverslips overnight, irradiated and fixed at indicated time after γ-radiation in PBS-4% paraformaldehyde for 20 min at RT, permeabilized in PBS with 0.2% Triton X-100 and blocked for at least 1 hours in PBS with

1% BSA. Incubation with anti-H3Ser10 and anti-γH2AX (Millipore) was performed overnight at 4°C, followed by anti-rabbit-AlexaFluor488 or anti-rabbit-AlexaFluor633 and anti-mouse-AlexaFluor633 staining, respectively. Incubation with fluorescein isothiocyanate (FITC)-conjugated monoclonal anti-α-tubulin antibody (Sigma) was performed for 2 hours at RT in PBS-1% BSA. Antibody incubation was followed by nuclear staining with 5 µg/ml Propidium Iodide (PI) in PBS for 20 min at RT. Coverslips were mounted in Mowiol 488 (Calbiochem-Novabiochem) containing 2.5% (w/v) 1,4-diazabicyclo (2,2,2) octane (DABCO, Sigma). For nuclear staining with DAPI, coverslips were mounted in Fluoroshield™ with DAPI (Sigma). The imaging was performed with a Nikon Eclipse Ti microscope.

4.8 Preparation of cell lysates, immunoprecipitation and immunoblotting.

To extract total proteins, cells were scraped on ice using cold RIPA buffer (150 mM NaCl; 50mM Tris HCl pH8; 0,1% SDS; 1% Igepal; 0,5% NP-40) plus a protease inhibitor cocktail (Complete™, Roche) and supplemented with 1 mM Na3VO4 (SIGMA), 10 mM NaF (SIGMA) and 1 mM DTT (SIGMA). Protein quantification was evaluated with Bradford (BIORAD) protein assay.

Immunoprecipitation (IP) experiments were performed using 0.1-0.4 mg of total lysate in HNTG buffer (20 mM HEPES, 150 mM NaCl, 10% Glycerol, 0.1% Triton X-100, protease inhibitor cocktail, 1 mM Na3VO4, 10 mM NaF and 1 mM DTT) with the specific primary antibodies, gently rocking overnight at 4 °C. A mix of protein A and protein G Sepharose 4 Fast Flow (Amersham Biosciences) was added for the last 2 hours of incubation. IPs were then washed six times in HNTG buffer and resuspended in 3× Laemmli Sample Buffer (5× Laemmli buffer composition: 50 mM Tris–HCl pH 6.8, 2% SDS, 10% glycerol, 0.05% bromophenol blue and 125 mM beta-mercaptoethanol). For immunoblot analysis, proteins were separated in 4-20% SDS-PAGE (Criterion Precast Gel, Biorad) or 10% SDS-PAGE and transferred to nitrocellulose membranes (GE Healthcare). Membranes were blocked with 5% not fat dried milk (NFDM) in TBS-0.1% Tween20 or in Odyssey Blocking Buffer (LI-COR, Biosciences) and incubated at 4°C ON with primary antibodies.

Then, membranes were washed in TBS-0.1% Tween20 and incubated 1 hour at RT with: mouse immunoglobulin G True Blot Ultra (Rockland) secondary horseradish peroxidase (HRP)-conjugated antibody or with HRP-proteinA (Invitrogen) secondary antibody for ECL detection (Claritytm Western ECL Substrate, BioRad Laboratories) following the

manufacturer's instructions or with conjugated secondary antibodies (AlexaFluor® 680, Invitrogen; IRDye 800, Rockland; IRDye-800CW; IRDye-680LT, Licor) for infrared detection (Odyssey Infrared Detection System, LI-COR).
Primary antibodies were purchase from Santa Cruz: p27 C-19 (sc-528), CDK1 (sc-54), cyclin B1 (sc-245), vinculin (sc-7649); BD Transduction Laboratories: p27kip1 (610242).

4.9 Kinase assay

For Kinase assay, cell lysates were immunoprecipitated using anti-CDK1 or control antibody, as described above. After 5 washes in HNTG buffer, one tenth of the IP was resuspended in kinase buffer (20 mM TrisHCl pH 6.8,10 mM MgCl2). Then, a kinase reaction solution containing the sample plus 50 µM ATP, γ-P32 ATP and 2 µg of H1-Histone as substrate in buffered solution (20 mM TrisHCl pH 6.8, 10 mM MgCl2) was prepared. The reaction was carried out at 30°C for 30 min and then 2X Laemmli sample buffer was added. After denaturation at 95°C for 10 minutes, proteins were loaded on a 4-20% SDS-PAGE (Criterion Precast Gel, Biorad). The gel was then dried and exposed on an autoradiographic film (GE, Amersham-Hyperfilm MP) at -80°C and developed after different time intervals. Band quantification was performed using Image Lab™ Software (Bio-Rad).

4.10 Statistical analyses

The computer software PRISM (version 4, GraphPad, Inc.) was used to make graphs and all statistical analyses. In all experiments, differences were considered significant when p was ≤0.05.

5 Discussion

From literature data and from studies carried on in our laboratory, it is well established that $p27^{kip1}$ is deeply involved in onset and prognosis of LBC. In this PhD project we decided to generate, characterize and use isogenic MCF-7 luminal B BC cells genetically modified for $p27^{kip1}$ by the ZFNs technology. We aimed to dissect the role of $p27^{kip1}$ and its mutations (considered as driver in LBC) in the oncogenic phenotypes of these cells, with a particular attention to their response to the most common therapies reserved to these patients.

We observed that loss of $p27^{kip1}$ or expression of the mutants K134fs and T171*, while having little effect on the proliferative rate of these cells in normal culture conditions, induced the acquisition of a more transformed phenotype, when evaluated in anchorage independence.

A crescent body of literature reports that $p27^{kip1}$ could play a role in the stem-like features of cells. In particular, Li and colleagues demonstrated a direct connection between $p27^{Kip1}$ and Sox2, one of the so called “Yamanaka factors” (Takahashi and Yamanaka, 2006). Consistently, our results in MCF-7 cells show that KO of $p27^{kip1}$ increases the stem-like properties of these BC cell line, both measured as mammosphere forming efficiency and as self-renewal capacity. Future *in vivo* experiments will assess whether this finding, coupled with the increased oncogenic potential observed in soft agar, will result in a significant increase of the tumor initiating potential of these cells.

A role for $p27^{Kip1}$ in the control of cell motility and migration has been reported. Expression of $p27^{Kip1}$ can stimulate the migration of cortical neurons and hepatocellular carcinoma cells (Besson, 2004; Itoh et al., 2007; Kawauchi, 2015; McAllister et al., 2003). Conversely, $p27^{Kip1}$ is reported to decrease migration and invasion of endothelial cells, vascular smooth muscle cells, mesangial cells, sarcoma cells and also normal mouse fibroblasts, especially when tested in 3D-context and in ECM-driven migration, (Baldassarre et al., 2005; Daniel et al., 2004; Goukassian, 2001; Sun et al., 2001). The data that we collected so far in MCF-7 cells indicate that loss of $p27^{kip1}$, or expression of $p27^{kip1}$ K134fs and T171* mutants, have no significant effects in 2D-motility assays, such as random motility and wound healing. However, testing the invasive behavior in 3D-context still need to be evaluated in this cellular model.

Our major goal was to evaluate whether loss of $p27^{kip1}$, or expression of $p27^{kip1}$ K134fs and T171* mutants impacted on the response of LBC to therapies that represent the standard of care for these patients, such as endocrine- and radiotherapy.

It is known that $p27^{Kip1}$KO mice show a higher susceptibility to genotoxic stimuli and to γ-radiation-induced tumors, displaying a decreased tumor-free survival, higher tumor

mortality and increased mitotic index, small/large scale genetic lesions and higher mutation frequency, effects that can be due, at least in part, to an inefficient G2/M checkpoint activation (Fero et al., 1998; Payne et al., 2008). Moreover, two different studies showed a direct correlation between low $p27^{Kip1}$ expression, cancer cells radioresistance and worse prognosis for esophageal carcinoma patients (Tong et al., 2011; Wang et al., 2012).

The effects of $p27^{kip1}$ loss following low doses of γ-radiation, particularly in LBC models, were still unexplored. Our results clearly indicate that expression of $p27^{kip1}$ is necessary for proper DNA damage response. Loss of $p27^{kip1}$ was associated to accumulation of residual DNA damage, followed by increased number of mitotic aberration. This DNA damage accumulation was however not associated with increased susceptibility to γ-radiation but, rather, with increased survival and accumulation of mitotic defects and genetic instability of MCF-7 cells.

Normal cells have evolved intricate checkpoint responses to preserve genomic integrity in response to DNA damage induced by γ-radiation. Cell cycle checkpoints take crucial part to these safeguard mechanisms, in order to exclude that a DNA damaged cell progresses and, eventually, divides. $p27^{kip1}$, as universal CDK inhibitor, has been involved in the DNA damage response and recent evidences directly link $p27^{kip1}$ downstream of ATM activation for the establishment of a G1-DNA damage checkpoint arrest (Cassimere et al., 2016). However, while this study finds that silencing of $p27^{kip1}$ (thus a partial reduction of the expression) led to increased susceptibility to γ-radiation, our experiments indicate that complete loss of $p27^{kip1}$ leads to increased survival of BC cells, possibly highlighting the disruption of further control mechanisms. In line with this possibility, our results point to a role of $p27^{kip1}$ in G2/M checkpoint, rather than in G1/S.

It is interesting to note that CDKN1B mutations found in LBC, such as the $p27^{kip1}$K134fs, which results in the loss of $p27^{kip1}$ C-terminal domain, include the loss of Ser140 of $p27^{kip1}$, controlled by ATM during DNA damage response (Cassimere et al., 2016). In line with this hypothesis, $p27^{kip1}$K134fs KI cells displayed in our analysis an intermediate behavior between the $p27^{kip1}$KO and $p27^{kip1}$ WT expressing clones. MCF-7 $p27^{kip1}$K134fs clones show a survival advantage in the clonogenic assays and a higher percentage of unsolved DSBs and defective mitoses after γ-radiations respect the control cells. However, the impact of $p27^{kip1}$K134fs on DNA damage repair and genomic instability seems to be lesser than the completely KO of $p27^{kip1}$. The K134fs mutation implicate the production of a

truncated form of $p27^{kip1}$ that could, in part, rescue the completely $p27^{kip1}$ null phenotype in this kind of treatment.

Genomic instability has potentially devastating effects and represents the hallmark of very aggressive cancers. Using highly controlled model system, we have highlighted the importance of $p27^{kip1}$ expression to preserve genomic integrity and to efficiently recognize and clear out aberrant cells after γ-radiation, if the damage cannot be solved. Since radiotherapy, with hormonal therapy, represents the standard of care for most LBC patients, our investigation provides potentially clinically relevant insights on the mechanisms underlying radioresistance.

The management of LBC considers as other gold standard treatment the estrogen-focused therapy, mainly with Tamoxifen. A large cohort of studies proved the efficacy of this drug in improving survival among women with early and advanced BC (Higgins and Baselga, 2011). However, although luminal B BC still express ER and ER-regulated genes, it seems to be more refractory to this kind of therapy (Tran and Bedard, 2011). Interestingly, clinical and functional studies demonstrate a link between $p27^{kip1}$ downregulation and LBC cells sensitivity to Tamoxifen (Cariou et al., 2000; Huh et al., 2016; Pohl, 2003; Porter et al., 2006). For this reason, we will also characterize and dissect the possible roles of $p27^{kip1}$ in the response to endocrine treatment in our luminal B BC model. These experiments are still in progress.

To overcome endocrine therapy resistance, a series of potential targets have been considered in luminal B BC, such as the IGFR1 signaling, the PI3K signaling, the FGFR1 signaling, the cell cycle (Tran and Bedard, 2011). Among them, considering that amplification of cyclin D1 and CDK4 is especially high in luminal B BC (Koboldt et al., 2012), one of the newest and most promising strategy to treat these tumors is targeting ER and the cell cycle. As future perspective, we will also investigate if the response to new generation of selective CDK4/6 inhibitors, such as Palbociclib, Ribociclib, and Abemaciclib, currently used for luminal B BC patients, could be affected by loss or mutation in $p27^{kip1}$.

References

Ades, F., Zardavas, D., Bozovic-Spasojevic, I., Pugliano, L., Fumagalli, D., de Azambuja, E., Viale, G., Sotiriou, C., and Piccart, M. (2014). Luminal B Breast Cancer: Molecular Characterization, Clinical Management, and Future Perspectives. J. Clin. Oncol. *32*, 2794–2803.

American Cancer Society (2015). Breast Cancer Facts & Figureures 2015-2016. Breast Cancer Facts Figure 2015-2016.

Baldassarre, G., Barone, M.V., Belletti, B., Sandomenico, C., Bruni, P., Spiezia, S., Boccia, A., Vento, M.T., Romano, A., Pepe, S., et al. (1999). Key role of the cyclin-dependent kinase inhibitor p27kip1 for embryonal carcinoma cell survival and differentiation. Oncogene *18*, 6241–6251.

Baldassarre, G., Belletti, B., Nicoloso, M.S., Schiappacassi, M., Vecchione, A., Spessotto, P., Morrione, A., Canzonieri, V., and Colombatti, A. (2005). p27Kip1-stathmin interaction influences sarcoma cell migration and invasion. Cancer Cell *7*, 51–63.

Barnes, A., Pinder, S., Bell, J., Paish, E., Wencyk, P., Robertson, J., Elston, C., and Ellis, I. (2003). Expression of p27kip1 in breast cancer and its prognostic significance. J. Pathol. *201*, 451–459.

Bediaga, N.G., Beristain, E., Calvo, B., Viguri, M.A., Gutierrez-Corres, B., Rezola, R., Ruiz-Diaz, I., Guerra, I., and de Pancorbo, M.M. (2016). Luminal B breast cancer subtype displays a dicotomic epigenetic pattern. SpringerPlus *5*.

Belletti, B., and Baldassarre, G. (2012). New light on p27 ^{kip1} in breast cancer. Cell Cycle *11*, 3701–3702.

Belletti, B., Nicoloso, M., Schiappacassi, M., Chimienti, E., Berton, S., Lovat, F., Colombatti, A., and Baldassarre, G. (2005). p27kip1 Functional Regulation in Human Cancer: A Potential Target for Therapeutic Designs. Curr. Med. Chem. *12*, 1589–1605.

Belletti, B., Nicoloso, M.S., Schiappacassi, M., Berton, S., Lovat, F., Wolf, K., Canzonieri, V., D'Andrea, S., Zucchetto, A., Friedl, P., et al. (2008). Stathmin Activity Influences Sarcoma Cell Shape, Motility, and Metastatic Potential. Mol. Biol. Cell *19*, 2003–2013.

Belletti, B., Pellizzari, I., Berton, S., Fabris, L., Wolf, K., Lovat, F., Schiappacassi, M., D'Andrea, S., Nicoloso, M.S., Lovisa, S., et al. (2010). p27kip1 Controls Cell Morphology and Motility by Regulating Microtubule-Dependent Lipid Raft Recycling. Mol. Cell. Biol. *30*, 2229–2240.

Besson, A. (2004). p27Kip1 modulates cell migration through the regulation of RhoA activation. Genes Dev. *18*, 862–876.

Besson, A. (2006). A pathway in quiescent cells that controls p27Kip1 stability, subcellular localization, and tumor suppression. Genes Dev. *20*, 47–64.

Boehm, M., Yoshimoto, T., Crook, M.F., Nallamshetty, S., True, A., Nabel, G.J., and Nabel, E.G. (2002). A growth factor-dependent nuclear kinase phosphorylates p27(Kip1) and regulates cell cycle progression. EMBO J. *21*, 3390–3401.

Bouwman, P., and Jonkers, J. (2012). The effects of deregulated DNA damage signalling on cancer chemotherapy response and resistance. Nat. Rev. Cancer *12*, 587–598.

Brenton, J.D. (2005). Molecular Classification and Molecular Forecasting of Breast Cancer: Ready for Clinical Application? J. Clin. Oncol. *23*, 7350–7360.

Buchholz, T.A. (2009). Radiation Therapy for Early-Stage Breast Cancer after Breast-Conserving Surgery. N. Engl. J. Med. *360*, 63–70.

Budach, W., B◆lke, E., and Matuschek, C. (2015). Hypofractionated Radiotherapy as Adjuvant Treatment in Early Breast Cancer. A Review and Meta-Analysis of Randomized Controlled Trials. Breast Care *10*, 240–245.
Burton, P.B.J., Raff, M.C., Kerr, P., Yacoub, M.H., and Barton, P.J.R. (1999). An Intrinsic Timer That Controls Cell-Cycle Withdrawal in Cultured Cardiac Myocytes. Dev. Biol. *216*, 659–670.
Cariou, S., Donovan, J.C.H., Flanagan, W.M., Milic, A., Bhattacharya, N., and Slingerland, J.M. (2000). Down-regulation of p21WAF1/CIP1 or p27Kip1 abrogates antiestrogen-mediated cell cycle arrest in human breast cancer cells. Proc. Natl. Acad. Sci. *97*, 9042–9046.
Cassimere, E.K., Mauvais, C., and Denicourt, C. (2016). p27Kip1 Is Required to Mediate a G1 Cell Cycle Arrest Downstream of ATM following Genotoxic Stress. PLOS ONE *11*, e0162806.
Chang, K., Creighton, C.J., Davis, C., Donehower, L., Drummond, J., Wheeler, D., Ally, A., Balasundaram, M., Birol, I., Butterfield, Y.S.N., et al. (2013). The Cancer Genome Atlas Pan-Cancer analysis project. Nat. Genet. *45*, 1113–1120.
Cheng, T. (2000). Hematopoietic Stem Cell Quiescence Maintained by p21cip1/waf1. Science *287*, 1804–1808.
Chu, I., Sun, J., Arnaout, A., Kahn, H., Hanna, W., Narod, S., Sun, P., Tan, C.-K., Hengst, L., and Slingerland, J. (2007). p27 Phosphorylation by Src Regulates Inhibition of Cyclin E-Cdk2. Cell *128*, 281–294.
Chu, I.M., Hengst, L., and Slingerland, J.M. (2008). The Cdk inhibitor p27 in human cancer: prognostic potential and relevance to anticancer therapy. Nat. Rev. Cancer *8*, 253–267.
Colleoni, M., and Munzone, E. (2015). Picking the optimal endocrine adjuvant treatment for pre-menopausal women. The Breast *24*, S11–S14.
Creighton, C. (2012). The molecular profile of luminal B breast cancer. Biol. Targets Ther. 289.
Cuadrado, M., Gutierrez-Martinez, P., Swat, A., Nebreda, A.R., and Fernandez-Capetillo, O. (2009). p27Kip1 Stabilization Is Essential for the Maintenance of Cell Cycle Arrest in Response to DNA Damage. Cancer Res. *69*, 8726–8732.
Daniel, C., Pippin, J., Shankland, S.J., and Hugo, C. (2004). The Rapamycin derivative RAD inhibits mesangial cell migration through the CDK-inhibitor p27KIP1. Lab. Invest. *84*, 588–596.
Deckbar, D., Jeggo, P.A., and Löbrich, M. (2011). Understanding the limitations of radiation-induced cell cycle checkpoints. Crit. Rev. Biochem. Mol. Biol. *46*, 271–283.
Ellis, M.J., Ding, L., Shen, D., Luo, J., Suman, V.J., Wallis, J.W., Van Tine, B.A., Hoog, J., Goiffon, R.J., Goldstein, T.C., et al. (2012). Whole-genome analysis informs breast cancer response to aromatase inhibition. Nature.
Ferlay, J., Soerjomataram, I., Dikshit, R., Eser, S., Mathers, C., Rebelo, M., Parkin, D.M., Forman, D., and Bray, F. (2015). Cancer incidence and mortality worldwide: Sources, methods and major patterns in GLOBOCAN 2012: Globocan 2012. Int. J. Cancer *136*, E359–E386.
Fero, M.L., Randel, E., Gurley, K.E., Roberts, J.M., and Kemp, C.J. (1998). The murine gene p27Kip1 is haplo-insufficient for tumour suppression. Nature *396*, 177–180.
Finn, R.S., Dering, J., Conklin, D., Kalous, O., Cohen, D.J., Desai, A.J., Ginther, C., Atefi, M., Chen, I., Fowst, C., et al. (2009). PD 0332991, a selective cyclin D kinase 4/6 inhibitor, preferentially inhibits proliferation of luminal estrogen receptor-positive human breast cancer cell lines in vitro. Breast Cancer Res. *11*, R77.
Finn, R.S., Crown, J.P., Lang, I., Boer, K., Bondarenko, I.M., Kulyk, S.O., Ettl, J., Patel, R., Pinter, T., Schmidt, M., et al. (2015). The cyclin-dependent kinase 4/6 inhibitor palbociclib

in combination with letrozole versus letrozole alone as first-line treatment of oestrogen receptor-positive, HER2-negative, advanced breast cancer (PALOMA-1/TRIO-18): a randomised phase 2 study. Lancet Oncol. *16*, 25–35.
Fujita, N. (2002). Akt-dependent Phosphorylation of p27Kip1 Promotes Binding to 14-3-3 and Cytoplasmic Localization. J. Biol. Chem. *277*, 28706–28713.
Gampenrieder, S.P., Rinnerthaler, G., and Greil, R. (2016). CDK4/6 inhibition in luminal breast cancer. Memo - Mag. Eur. Med. Oncol. *9*, 76–81.
Gao, F.-B., Durand, B., and Raff, M. (1997). Oligodendrocyte precursor cells count time but not cell divisions before differentiation. Curr. Biol. *7*, 152–155.
Gillett, C.E., Smith, P., Peters, G., Lu, X., and Barnes, D.M. (1999). Cyclin-dependent kinase inhibitor p27Kip1 expression and interaction with other cell cycle-associated proteins in mammary carcinoma. J. Pathol. *187*, 200–206.
Goldhirsch, A., Wood, W.C., Coates, A.S., Gelber, R.D., Thurlimann, B., Senn, H.-J., and Panel members (2011). Strategies for subtypes--dealing with the diversity of breast cancer: highlights of the St Gallen International Expert Consensus on the Primary Therapy of Early Breast Cancer 2011. Ann. Oncol. *22*, 1736–1747.
Goukassian, D. (2001). Overexpression of p27Kip1 by doxycycline-regulated adenoviral vectors inhibits endothelial cell proliferation and migration and impairs angiogenesis. FASEB J. *15*, 1877–1885.
Grimmler, M., Wang, Y., Mund, T., Cilenšek, Z., Keidel, E.-M., Waddell, M.B., Jäkel, H., Kullmann, M., Kriwacki, R.W., and Hengst, L. (2007). Cdk-Inhibitory Activity and Stability of p27Kip1 Are Directly Regulated by Oncogenic Tyrosine Kinases. Cell *128*, 269–280.
Gu, G., Dustin, D., and Fuqua, S.A. (2016). Targeted therapy for breast cancer and molecular mechanisms of resistance to treatment. Curr. Opin. Pharmacol. *31*, 97–103.
Guan, X., Wang, Y., Xie, R., Chen, L., Bai, J., Lu, J., and Kuo, M.T. (2010). p27Kip1 as a prognostic factor in breast cancer: a systematic review and meta-analysis. J. Cell. Mol. Med. *14*, 944–953.
Hara, T., Kamura, T., Nakayama, K., Oshikawa, K., Hatakeyama, S., and Nakayama, K. (2001). Degradation of p27(Kip1) at the G(0)-G(1) transition mediated by a Skp2-independent ubiquitination pathway. J. Biol. Chem. *276*, 48937–48943.
Harbeck, N., and Gnant, M. (2016). Breast cancer. The Lancet.
Hartwell, L.H., and Weinert, T.A. (1989). Checkpoints: controls that ensure the order of cell cycle events. Science *246*, 629–634.
Hauck, L., Harms, C., Rohne, J., Gertz, K., Dietz, R., Endres, M., and von Harsdorf, R. (2008). Protein kinase CK2 links extracellular growth factor signaling with the control of p27Kip1 stability in the heart. Nat. Med. *14*, 315–324.
Higgins, M.J., and Baselga, J. (2011). Targeted therapies for breast cancer. J. Clin. Invest. *121*, 3797–3803.
Huh, S.J., Oh, H., Peterson, M.A., Almendro, V., Hu, R., Bowden, M., Lis, R.L., Cotter, M.B., Loda, M., Barry, W.T., et al. (2016). The Proliferative Activity of Mammary Epithelial Cells in Normal Tissue Predicts Breast Cancer Risk in Premenopausal Women. Cancer Res. *76*, 1926–1934.
Ignatiadis, M., and Sotiriou, C. (2013). Luminal breast cancer: from biology to treatment. Nat. Rev. Clin. Oncol. *10*, 494–506.
Iliakis, G., Wang, Y., Guan, J., and Wang, H. (2003). DNA damage checkpoint control in cells exposed to ionizing radiation. Oncogene *22*, 5834–5847.
Ishida, N., Kitagawa, M., Hatakeyama, S., and Nakayama, K. (2000). Phosphorylation at serine 10, a major phosphorylation site of p27(Kip1), increases its protein stability. J. Biol. Chem. *275*, 25146–25154.
Israels, E.D. (2000). The Cell Cycle. The Oncologist *5*, 510–513.
Itoh, Y., Masuyama, N., Nakayama, K., Nakayama, K.I., and Gotoh, Y. (2007). The Cyclin-

dependent Kinase Inhibitors p57 and p27 Regulate Neuronal Migration in the Developing Mouse Neocortex. J. Biol. Chem. *282*, 390–396.
James, M.K., Ray, A., Leznova, D., and Blain, S.W. (2008). Differential Modification of p27Kip1 Controls Its Cyclin D-cdk4 Inhibitory Activity. Mol. Cell. Biol. *28*, 498–510.
Jiang, Y.-Z., Yu, K.-D., Zuo, W.-J., Peng, W.-T., and Shao, Z.-M. (2014). *GATA3* mutations define a unique subtype of luminal-like breast cancer with improved survival: *GATA3* Mutations in Breast Cancer. Cancer *120*, 1329–1337.
Kamura, T., Hara, T., Matsumoto, M., Ishida, N., Okumura, F., Hatakeyama, S., Yoshida, M., Nakayama, K., and Nakayama, K.I. (2004). Cytoplasmic ubiquitin ligase KPC regulates proteolysis of p27(Kip1) at G1 phase. Nat. Cell Biol. *6*, 1229–1235.
Kawauchi, T. (2015). Cellullar insights into cerebral cortical development: focusing on the locomotion mode of neuronal migration. Front. Cell. Neurosci. *9*.
Kinner, A., Wu, W., Staudt, C., and Iliakis, G. (2008). -H2AX in recognition and signaling of DNA double-strand breaks in the context of chromatin. Nucleic Acids Res. *36*, 5678–5694.
Koboldt, D.C., Fulton, R.S., McLellan, M.D., Schmidt, H., Kalicki-Veizer, J., McMichael, J.F., Fulton, L.L., Dooling, D.J., Ding, L., Mardis, E.R., et al. (2012). Comprehensive molecular portraits of human breast tumours. Nature *490*, 61–70.
Kotoshiba, S., Kamura, T., Hara, T., Ishida, N., and Nakayama, K.I. (2005). Molecular Dissection of the Interaction between p27 and Kip1 Ubiquitylation-promoting Complex, the Ubiquitin Ligase That Regulates Proteolysis of p27 in G1 Phase. J. Biol. Chem. *280*, 17694–17700.
Langlands, F.E., Horgan, K., Dodwell, D.D., and Smith, L. (2013). Breast cancer subtypes: response to radiotherapy and potential radiosensitisation. Br. J. Radiol. *86*, 20120601.
Lee, M.K., Varzi, L.A., Chung, D.U., Cao, M., Gornbein, J., Apple, S.K., and Chang, H.R. (2015). The Effect of Young Age in Hormone Receptor Positive Breast Cancer. BioMed Res. Int. *2015*, 1–6.
Lee-Hoeflich, S.T., Pham, T.Q., Dowbenko, D., Munroe, X., Lee, J., Li, L., Zhou, W., Haverty, P.M., Pujara, K., Stinson, J., et al. (2011). PPM1H Is a p27 Phosphatase Implicated in Trastuzumab Resistance. Cancer Discov. *1*, 326–337.
Li, H., Collado, M., Villasante, A., Matheu, A., Lynch, C.J., Cañamero, M., Rizzoti, K., Carneiro, C., Martínez, G., Vidal, A., et al. (2012). p27Kip1 Directly Represses Sox2 during Embryonic Stem Cell Differentiation. Cell Stem Cell *11*, 845–852.
Liang, J., Zubovitz, J., Petrocelli, T., Kotchetkov, R., Connor, M.K., Han, K., Lee, J.-H., Ciarallo, S., Catzavelos, C., Beniston, R., et al. (2002). PKB/Akt phosphorylates p27, impairs nuclear import of p27 and opposes p27-mediated G1 arrest. Nat. Med. *8*, 1153–1160.
Linee Guida AIOM 2015 Neoplasie della mammella. Edizione 2015.
Loi, S., Haibe-Kains, B., Majjaj, S., Lallemand, F., Durbecq, V., Larsimont, D., Gonzalez-Angulo, A.M., Pusztai, L., Symmans, W.F., Bardelli, A., et al. (2010). PIK3CA mutations associated with gene signature of low mTORC1 signaling and better outcomes in estrogen receptor-positive breast cancer. Proc. Natl. Acad. Sci. *107*, 10208–10213.
Lord, C.J., and Ashworth, A. (2012). The DNA damage response and cancer therapy. Nature *481*, 287–294.
Matsu-ura, T., Sasaki, H., Okada, M., Mikoshiba, K., and Ashraf, M. (2016). Attenuation of teratoma formation by p27 overexpression in induced pluripotent stem cells. Stem Cell Res. Ther. *7*.
Maucuer, A., Moreau, J., Méchali, M., and Sobel, A. (1993). Stathmin gene family: phylogenetic conservation and developmental regulation in Xenopus. J. Biol. Chem. *268*, 16420–16429.
McAllister, S.S., Becker-Hapak, M., Pintucci, G., Pagano, M., and Dowdy, S.F. (2003). Novel p27kip1 C-Terminal Scatter Domain Mediates Rac-Dependent Cell Migration

Independent of Cell Cycle Arrest Functions. Mol. Cell. Biol. *23*, 216–228.
Miller, E., Lee, H.J., Lulla, A., Hernandez, L., Gokare, P., and Lim, B. (2014). Current treatment of early breast cancer: adjuvant and neoadjuvant therapy. F1000Research.
Miller, T.W., Balko, J.M., and Arteaga, C.L. (2011). Phosphatidylinositol 3-Kinase and Antiestrogen Resistance in Breast Cancer. J. Clin. Oncol. *29*, 4452–4461.
Mohamed, A., Krajewski, K., Cakar, B., and Ma, C.X. (2013). Targeted Therapy for Breast Cancer. Am. J. Pathol. *183*, 1096–1112.
Nahta, R. (2004). P27kip1 Down-Regulation Is Associated with Trastuzumab Resistance in Breast Cancer Cells. Cancer Res. *64*, 3981–3986.
Nakayama, K., Ishida, N., Shirane, M., Inomata, A., Inoue, T., Shishido, N., Horii, I., Loh, D.Y., and Nakayama, K. (1996). Mice lacking p27(Kip1) display increased body size, multiple organ hyperplasia, retinal dysplasia, and pituitary tumors. Cell *85*, 707–720.
Nakayama, K., Nagahama, H., Minamishima, Y.A., Miyake, S., Ishida, N., Hatakeyama, S., Kitagawa, M., Iemura, S., Natsume, T., and Nakayama, K.I. (2004). Skp2-Mediated Degradation of p27 Regulates Progression into Mitosis. Dev. Cell *6*, 661–672.
Newman, L., Xia, W., Yang, H.Y., Sahin, A., Bondy, M., Lukmanji, F., Hung, M.C., and Lee, M.H. (2001). Correlation of p27 protein expression with HER-2/neu expression in breast cancer. Mol. Carcinog. *30*, 169–175.
Nguyen, L. (2006). p27kip1 independently promotes neuronal differentiation and migration in the cerebral cortex. Genes Dev. *20*, 1511–1524.
Nguyen, L., Besson, A., Roberts, J.M., and Guillemot, F. (2006). Coupling Cell Cycle Exit, Neuronal Differentiation and Migration in Cortical Neurogenesis. Cell Cycle *5*, 2314–2318.
Nurse, P. (2000). A Long Twentieth Century of the Cell Cycle and Beyond. Cell *100*, 71–78.
O'Connor, M.J. (2015). Targeting the DNA Damage Response in Cancer. Mol. Cell *60*, 547–560.
Pawlik, T.M., and Keyomarsi, K. (2004). Role of cell cycle in mediating sensitivity to radiotherapy. Int. J. Radiat. Oncol. *59*, 928–942.
Payne, S.R., Zhang, S., Tsuchiya, K., Moser, R., Gurley, K.E., Longton, G., deBoer, J., and Kemp, C.J. (2008). p27kip1 Deficiency Impairs G2/M Arrest in Response to DNA Damage, Leading to an Increase in Genetic Instability. Mol. Cell. Biol. *28*, 258–268.
Perou, C.M., Sørlie, T., Eisen, M.B., van de Rijn, M., Jeffrey, S.S., Rees, C.A., Pollack, J.R., Ross, D.T., Johnsen, H., Akslen, L.A., et al. (2000). Molecular portraits of human breast tumours. Nature *406*, 747–752.
Philipp-Staheli, J., Payne, S.R., and Kemp, C.J. (2001). p27Kip1: Regulation and Function of a Haploinsufficient Tumor Suppressor and Its Misregulation in Cancer. Exp. Cell Res. *264*, 148–168.
Pohl, G. (2003). High p27Kip1 Expression Predicts Superior Relapse-Free and Overall Survival for Premenopausal Women With Early-Stage Breast Cancer Receiving Adjuvant Treatment With Tamoxifen Plus Goserelin. J. Clin. Oncol. *21*, 3594–3600.
Porter, P.L., Barlow, W.E., Yeh, I.-T., Lin, M.G., Yuan, X.P., Donato, E., Sledge, G.W., Shapiro, C.L., Ingle, J.N., Haskell, C.M., et al. (2006). p27Kip1 and Cyclin E Expression and Breast Cancer Survival After Treatment With Adjuvant Chemotherapy. JNCI J. Natl. Cancer Inst. *98*, 1723–1731.
Rodier, G., Montagnoli, A., Di Marcotullio, L., Coulombe, P., Draetta, G.F., Pagano, M., and Meloche, S. (2001). p27 cytoplasmic localization is regulated by phosphorylation on Ser10 and is not a prerequisite for its proteolysis. EMBO J. *20*, 6672–6682.
Roskoski, R. (2016). Cyclin-dependent protein kinase inhibitors including palbociclib as anticancer drugs. Pharmacol. Res. *107*, 249–275.
Rubin, C.I., and Atweh, G.F. (2004). The role of stathmin in the regulation of the cell cycle. J. Cell. Biochem. *93*, 242–250.

Russo, A.A., Jeffrey, P.D., Patten, A.K., Massagué, J., and Pavletich, N.P. (1996). Crystal structure of the p27Kip1 cyclin-dependent-kinase inibitor bound to the cyclin A–Cdk2 complex. Nature *382*, 325–331.
Santivasi, W.L., and Xia, F. (2014). Ionizing Radiation-Induced DNA Damage, Response, and Repair. Antioxid. Redox Signal. *21*, 251–259.
Schiappacassi, M., Lovisa, S., Lovat, F., Fabris, L., Colombatti, A., Belletti, B., and Baldassarre, G. (2011). Role of T198 Modification in the Regulation of p27Kip1 Protein Stability and Function. PLoS ONE *6*, e17673.
Segatto, I., Berton, S., Sonego, M., Massarut, S., Perin, T., Piccoli, E., Colombatti, A., Vecchione, A., Baldassarre, G., and Belletti, B. (2014). Surgery-induced wound response promotes stem-like and tumor-initiating features of breast cancer cells, <i>via</i> STAT3 signaling. Oncotarget *5*, 6267–6279.
Serres, M.P., Kossatz, U., Chi, Y., Roberts, J.M., Malek, N.P., and Besson, A. (2012). p27Kip1 controls cytokinesis via the regulation of citron kinase activation. J. Clin. Invest. *122*, 844–858.
Sharma, S.S., Ma, L., Bagui, T.K., Forinash, K.D., and Pledger, W.J. (2012). A p27Kip1 mutant that does not inhibit CDK activity promotes centrosome amplification and micronucleation. Oncogene *31*, 3989–3998.
Shaw, F.L., Harrison, H., Spence, K., Ablett, M.P., Simões, B.M., Farnie, G., and Clarke, R.B. (2012). A Detailed Mammosphere Assay Protocol for the Quantification of Breast Stem Cell Activity. J. Mammary Gland Biol. Neoplasia *17*, 111–117.
Sheaff, R.J., Groudine, M., Gordon, M., Roberts, J.M., and Clurman, B.E. (1997). Cyclin E-CDK2 is a regulator of p27Kip1. Genes Dev. *11*, 1464–1478.
Sherr, C.J., and Roberts, J.M. (1999). CDK inhibitors: positive and negative regulators of G1-phase progression. Genes Dev. *13*, 1501–1512.
Shin, I., Yakes, F.M., Rojo, F., Shin, N.-Y., Bakin, A.V., Baselga, J., and Arteaga, C.L. (2002). PKB/Akt mediates cell-cycle progression by phosphorylation of p27Kip1 at threonine 157 and modulation of its cellular localization. Nat. Med. *8*, 1145–1152.
Smid, M., Wang, Y., Zhang, Y., Sieuwerts, A.M., Yu, J., Klijn, J.G.M., Foekens, J.A., and Martens, J.W.M. (2008). Subtypes of Breast Cancer Show Preferential Site of Relapse. Cancer Res. *68*, 3108–3114.
Sorlie, T., Perou, C.M., Tibshirani, R., Aas, T., Geisler, S., Johnsen, H., Hastie, T., Eisen, M.B., van de Rijn, M., Jeffrey, S.S., et al. (2001). Gene expression patterns of breast carcinomas distinguish tumor subclasses with clinical implications. Proc. Natl. Acad. Sci. *98*, 10869–10874.
Sorlie, T., Tibshirani, R., Parker, J., Hastie, T., Marron, J.S., Nobel, A., Deng, S., Johnsen, H., Pesich, R., Geisler, S., et al. (2003). Repeated observation of breast tumor subtypes in independent gene expression data sets. Proc. Natl. Acad. Sci. *100*, 8418–8423.
Spataro, V.J., Litman, H., Viale, G., Maffini, F., Masullo, M., Golouh, R., Martinez-Tello, F.J., Grigolato, P., Shilkin, K.B., Gusterson, B.A., et al. (2003). Decreased immunoreactivity for p27 protein in patients with early-stage breast carcinoma is correlated with HER-2/ *neu* overexpression and with benefit from one course of perioperative chemotherapy in patients with negative lymph node status: Results from International Breast Cancer Study Group Trial V. Cancer *97*, 1591–1600.
Speers, C., and Pierce, L.J. (2016). Postoperative Radiotherapy After Breast-Conserving Surgery for Early-Stage Breast Cancer: A Review. JAMA Oncol. *2*, 1075.
Spirin, K.S., Simpson, J.F., Takeuchi, S., Kawamata, N., Miller, C.W., and Koeffler, H.P. (1996). p27/Kip1 mutation found in breast cancer. Cancer Res. *56*, 2400–2404.
Stephens, P.J., Tarpey, P.S., Davies, H., Van Loo, P., Greenman, C., Wedge, D.C., Zainal, S.N., Martin, S., Varela, I., Bignell, G.R., et al. (2012). The landscape of cancer genes and mutational processes in breast cancer. Nature.

Sugihara, E. (2006). Suppression of Centrosome Amplification after DNA Damage Depends on p27 Accumulation. Cancer Res. *66*, 4020–4029.
Sun, J., Marx, S.O., Chen, H.-J., Poon, M., Marks, A.R., and Rabbani, L.E. (2001). Role for p27Kip1 in Vascular Smooth Muscle Cell Migration. Circulation *103*, 2967–2972.
Susaki, E., and Nakayama, K.I. (2007). Multiple Mechanisms for p27 ^{Kip1} Translocation and Degradation. Cell Cycle *6*, 3015–3020.
Takahashi, K., and Yamanaka, S. (2006). Induction of Pluripotent Stem Cells from Mouse Embryonic and Adult Fibroblast Cultures by Defined Factors. Cell *126*, 663–676.
Tapia, J.C., Bolanos-Garcia, V.M., Sayed, M., Allende, C.C., and Allende, J.E. (2004). Cell cycle regulatory protein p27KIP1 is a substrate and interacts with the protein kinase CK2. J. Cell. Biochem. *91*, 865–879.
Tong, Q., Zhang, W., Jin, S., Li, S., and Chen, Z. (2011). The relationship between p27 ^{kip1} expression and the change of radiosensitivity of esophageal carcinoma cells. Scand. J. Gastroenterol. *46*, 173–176.
Toyoshima, H., and Hunter, T. (1994). p27, a novel inhibitor of G1 cyclin-Cdk protein kinase activity, is related to p21. Cell *78*, 67–74.
Tran, B., and Bedard, P.L. (2011). Luminal-B breast cancer and novel therapeutic targets. Breast Cancer Res. *13*, 221.
Vervoorts, J., and Lüscher, B. (2008). Post-translational regulation of the tumor suppressor p27KIP1. Cell. Mol. Life Sci. *65*, 3255–3264.
Viale, G. (2012). The current state of breast cancer classification. Ann. Oncol. *23*, x207–x210.
Viglietto, G., Motti, M.L., Bruni, P., Melillo, R.M., D'Alessio, A., Califano, D., Vinci, F., Chiappetta, G., Tsichlis, P., Bellacosa, A., et al. (2002). Cytoplasmic relocalization and inhibition of the cyclin-dependent kinase inhibitor p27Kip1 by PKB/Akt-mediated phosphorylation in breast cancer. Nat. Med. *8*, 1136–1144.
Vlach, J. (1997). Phosphorylation-dependent degradation of the cyclin-dependent kinase inhibitor p27Kip1. EMBO J. *16*, 5334–5344.
Vlach, J., Hennecke, S., Alevizopoulos, K., Conti, D., and Amati, B. (1996). Growth arrest by the cyclin-dependent kinase inhibitor p27Kip1 is abrogated by c-Myc. EMBO J. *15*, 6595–6604.
Wang, X.-C., Tian, L.-L., Tian, J., and Jiang, X.-Y. (2012). Overexpression of SKP2 promotes the radiation resistance of esophageal squamous cell carcinoma. Radiat. Res. *177*, 52–58.
Wardell, S.E., Ellis, M.J., Alley, H.M., Eisele, K., VanArsdale, T., Dann, S.G., Arndt, K.T., Primeau, T., Griffin, E., Shao, J., et al. (2015). Efficacy of SERD/SERM Hybrid-CDK4/6 Inhibitor Combinations in Models of Endocrine Therapy-Resistant Breast Cancer. Clin. Cancer Res. *21*, 5121–5130.
Wolf, G., Reinking, R., Zahner, G., Stahl, R.A.K., and Shankland, S.J. (2003). Erk 1,2 phosphorylates p27 Kip1 : Functional evidence for a role in high glucose-induced hypertrophy of mesangial cells. Diabetologia *46*, 1090–1099.
Yoon, N.K., Maresh, E.L., Shen, D., Elshimali, Y., Apple, S., Horvath, S., Mah, V., Bose, S., Chia, D., Chang, H.R., et al. (2010). Higher levels of GATA3 predict better survival in women with breast cancer. Hum. Pathol. *41*, 1794–1801.
Zhao, H., Faltermeier, C.M., Mendelsohn, L., Porter, P.L., Clurman, B.E., and Roberts, J.M. (2015). Mislocalization of p27 to the cytoplasm of breast cancer cells confers resistance to anti-HER2 targeted therapy. Oncotarget *5*, 12704–12714.
(2005). Effects of chemotherapy and hormonal therapy for early breast cancer on recurrence and 15-year survival: an overview of the randomised trials. The Lancet *365*, 1687–1717.